PENNSTATE 1855

DEPARTMENT OF METEOROLOGY
COLLEGE OF EARTH AND MINERAL SCIENCES

Tom's Influence and Inspiration in Today's Numerical Weather Prediction at PSU

The Warner Memorial Symposium

NCAR Foothills Lab
Boulder, CO
2 December 2011

David R. Stauffer, PSU

PENNSTATE

1 8 5 5

Outline

- Some memories of my early grad student years starting in 1981
- Some highlights of my PSU Numerical Weather Prediction (NWP) Group activities over the last ten years
  - – NWP for Air Quality Modeling
  - – Military-Defense-Aviation NWP Systems
    - Army, Marines, DTRA, NOAA
  - – Basic and Applied Research
    - Stable Boundary Layer, Waves and AT&D
    - Model Ensembles
      - – Advanced Data Assimilation
      - – Uncertainty Quantification

PENNSTATE

1 8 5 5

A Numerical Study of Appalachian Cold-Air Damming and Coastal Frontogenesis

DAVID R. STAUFFER AND THOMAS T. WARNER

Department of Meteorology, The Pennsylvania State University, University Park, PA 16802

(Manuscript received 28 March 1986, in final form 9 October 1986)

ABSTRACT

A 24-h numerical simulation is used to study features of the wedge-shaped pressure ridge and the coastal front, which occur in eastern United States during winter and often cause substantial errors in operational models. Specifically, the Penn State/National Center for Atmospheric Research, Mesoscale Model (MM) is used as a diagnostic tool to investigate the mesoscale structure of these phenomena associated with the Appalachian ice-storm of 13–14 January 1980.

The MM, which used 15 vertical levels (8 below 800 mb), a 50-km, horizontal mesh size, and a multi-level boundary-layer parameterization, produced a better forecast of boundary-layer temperature and sea-level pressure than did the National Meteorological Center's operational model for this case-study period. To the east of the mountains, the MM maintained the wedge-ridge pattern and produced the low-level, northerly flow which is characteristic of the damming region. The MM also provided reasonable vertical profiles of temperature and wind, including a low-level, mountain-parallel jet which is commonly observed along mountain ridges during cold-air damming. However, despite the model's fairly sophisticated surface energy equation and moderate spatial resolution, the low-level temperature simulation was still 1–5°C too warm in some areas to the east of the mountains.

The moderate horizontal and vertical resolution did allow the MM to develop the coastal front which appeared in the Chesapeake Bay–New Jersey area by the end of the 24-h study period. Despite the small-scale nature of a coastal front, synoptic and mesoalpha-scale forcing in the model created a realistic, coastal baroclinic zone. The simulated, low-level temperature gradient and convergence zone compared favorably with surface observations. The simulated coastal front, separating easterly maritime air from the cold northerly flow inland, diminished in strength with height and disappeared by 940 mb. In the damming region, observations suggested and model results showed an "extended coastal front": a sloping inversion separating the trapped surface-based cold air from the warm onshore flow above. This feature appears to be at least partially responsible for the low-level jet.

Model-generated, kinematic trajectories showed the strongly sheared, three-dimensional character of the flow within the damming region. These model results and observations indicate that a relatively large number of model layers would be required below ~800 mb in order to adequately model the thermal and wind field structures.

1. Introduction

The veteran forecaster raises his brow whenever a strong surface anticyclone, tracking eastward toward New England, extends southward along the eastern slopes of the Appalachians as an inverted ridge in the sea-level pressure (SLP). This familiar "wedge ridge," the result of cold-air "damming" by the mountains, is often the harbinger of hazardous winter weather east of the Appalachian Mountain chain.

Despite the sufficient horizontal grid spacing to resolve the wedge ridge in current operational models, the incomplete treatment of the boundary-layer processes generally contributes to poor mass-field and wind-field forecasts in the damming region, while forecast errors are normally much smaller elsewhere on the model domain (Richwien, 1980; Bosart, 1981; Forbes et al., 1987). East of the mountains, boundary-layer temperatures are often predicted to be too warm, while surface pressures are forecast to fall too rapidly.

This wedge-shaped pressure ridge is often associated with yet another forecast challenge existing along certain parts of the east coast of the United States. Bosart et al. (1972) and Bosart (1975) have studied a shallow, pseudo-warm or stationary "coastal front" in New England. The observation that coastal fronts tend to be oriented more parallel to the terrain contours than to the coastline may support the hypothesis that cold-air damming enhances their intensity (Richwien, 1980). Furthermore, Bosart (1981), among others, indicates that this cold-air pressure ridge also favors coastal cyclogenesis.

This paper discusses the results of a numerical simulation, which used a mesoscale model (MM) with sophisticated boundary-layer physics and moderate horizontal and vertical resolution, to investigate the mesoscale detail of the wedge ridge and coastal front. The case studied is the Appalachian freezing-rain event of 13–14 January 1980, recently documented by Forbes et al. (1987).

DEPARTMENT OF

METEOROLOGY

COLLEGE OF EARTH AND MINERAL SCIENCES

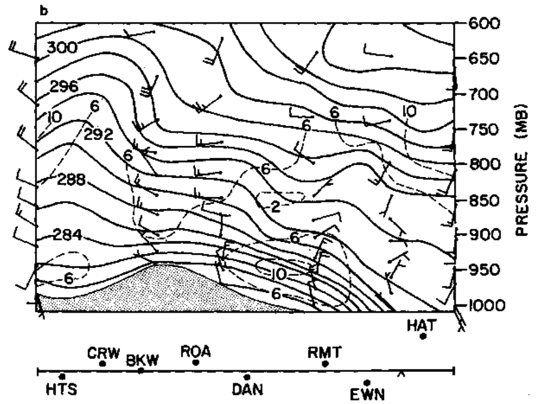

FIG. 17b. As in Fig. 16a but from 24-h forecast verifying at 1200 UTC 14 January 1980.

the wind-field forecast at 1200 UTC 14 January verifies reasonably well against the available data, no wind data were available at this time above the surface at GSO. The predicted *surface* wind for this time at GSO compares favorably with the observed 6 m s^{-1} wind from the north-northeast. Observed low-level winds at IAD and AHN at this time were 3–5 m s^{-1} from the northeast.

The dynamical arguments of Schwerdtfeger mentioned earlier, that attempt to explain the existence of terrain-induced jets in terms of geostrophic considerations, can be useful here. That is, the presence of the extended coastal-front inversion in the damming region may accelerate the air toward the south, along the eastern Appalachian slope. Perhaps the underestimation of the inversion strength by the model may explain why the *simulated* low-level jet appeared 4–8 h after it was observed. Geostrophic forcing would be weaker and therefore more time would be required for the model to develop the jet. Forbes et al. (1987) state that the *observations* in this case were generally supportive of Schwerdtfeger's arguments.

Figure 19 shows a back trajectory of an air parcel which was embedded in the jet core at 950 mb at 24 h in the numerical simulation. This trajectory and those presented later were calculated from the three-dimensional wind fields defined at 15-min intervals by the 24-h model simulation. The dark dots in Fig. 19 show the parcel's position at 2-h intervals with the total wind T, ageostrophic wind A and geostrophic wind G plotted every 4 h. The pressure level and pressure height of the parcel above the surface are in millibars and enclosed in parentheses. The parcel's mean speed for each 2-h interval is in meters per second and is encircled.

The parcel, which originated in the low levels over the ocean surface, initially accelerates and then turns westward after 8 h (2000 UTC 13 January). Near the coast, its motion is largely geostrophic. At this time (0200 UTC 14 January), the coastal front has not developed yet; but the parcel still rises and decelerates as it moves further inland over the cold air. As it ascends, it passes through different pressure-gradient regimes. After 18 h, owing to the stability of the air, the parcel is deflected to the left (south) as predicted by Schwerdtfeger's argument. The local pressure gradient force is directed normal to and away from the mountains. During the next few hours, Coriolis effects become important enough to support the geostrophic-type flow of the northerly jet. An analysis of other trajectories in the region of the jet at 24 h produced similar results. Examination of the low-level wind simulation in the region of this trajectory shows reasonable agreement with available observations. Therefore, its general characteristics should be representative of the true atmosphere.

d. The coastal front

The initial surface-layer temperature field at 1200 UTC 13 January was shown in Fig. 7 to have isotherms oriented nearly east–west in the coastal states; little or no low-level convergence existed in the initial model winds at this time along the coast. By 0400 UTC 14 January, the model produced a weak convergence zone in the Chesapeake Bay–New Jersey area (Fig. 10), where the coastal front was just beginning to develop. By 1200 UTC, a mesoscale temperature gradient and a strong convergence zone were well developed in this

Omaha NWP Conference 1983

PENNSTATE

Montreal NWP Conference 1985

DEPARTMENT OF
METEOROLOGY
COLLEGE OF EARTH AND
MINERAL SCIENCES

Denver NWP Conference 1991

PENNSTATE

Current and Recent NWP and Process Studies for Air Quality Applications…

- Alaska PM2.5: EPA and Alaska Department of Environmental Conservation (ADEC), Gaudet
- California Ozone and PM2.5: Bay Area Air Quality Management District (BAAQMD), Deng and Rogers

Alaska Winter Case – PM2.5

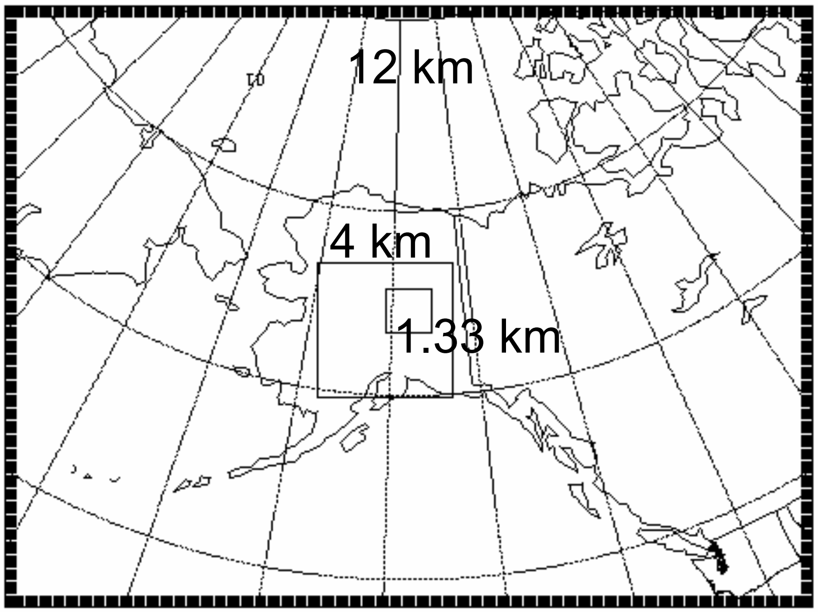

1.33 km Domain

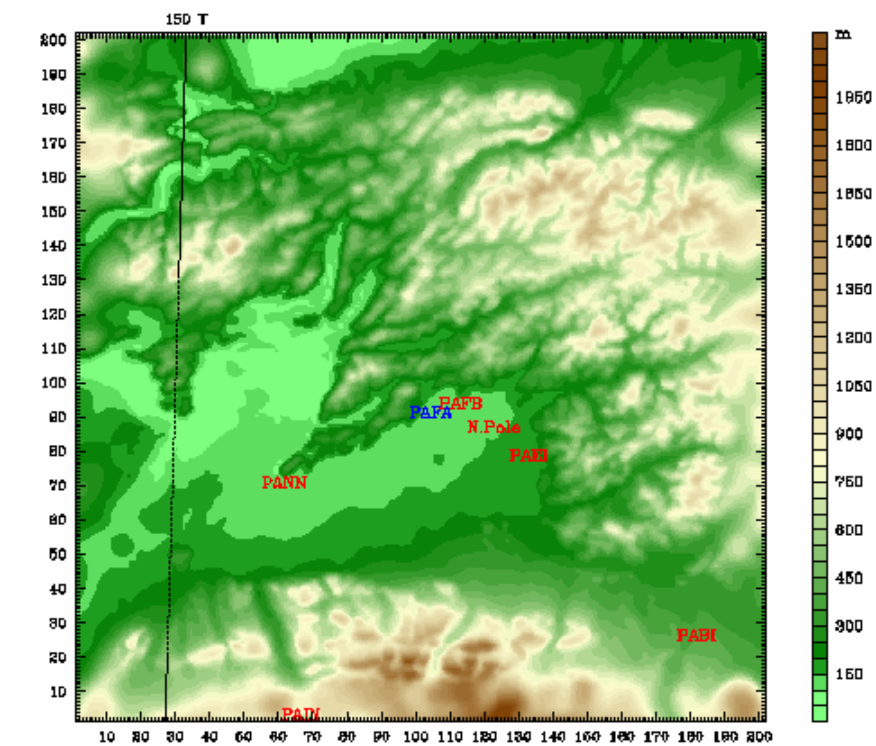

Alaska Domains:

12 km:	Synoptic scale	401 x 301	Δt = 24 s
4 km:	Central AK region	202 x 202	Δt = 8 s
1.33 km:	Tanana Basin	202 x 202	Δt = 4 s

39 vertical levels, to 4 m grid spacing near surface

California Summer Case - Ozone

WRF Streamlines with Terrain Shaded

Daytime: 0000UTC 30 July 2000

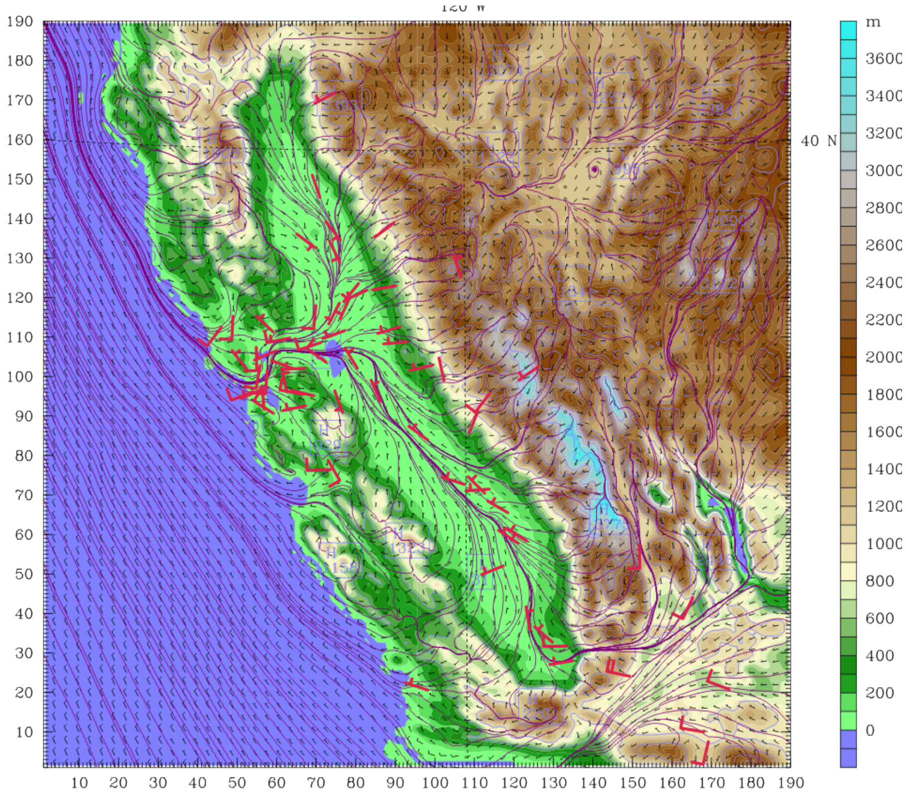

Multiscale FDDA – Analysis nudging on 36- and 12-km domains, obs nudging on 12- and 4-km domains

Schematic Diagram of Typical Regional Daytime Flow

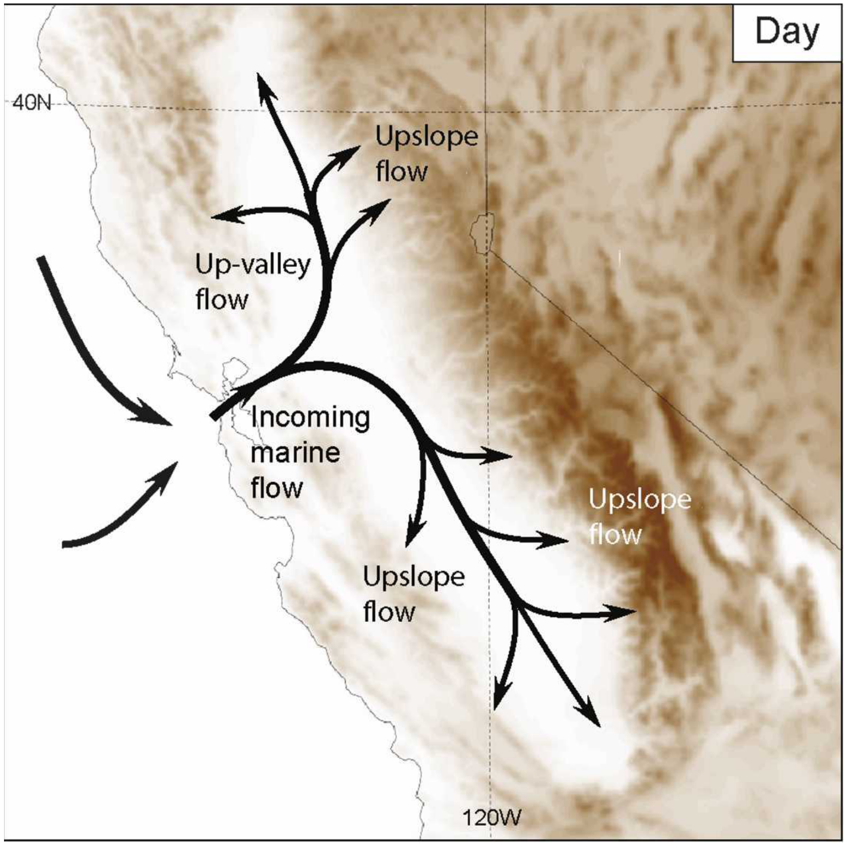

After Bao et al. (2008), Stauffer (1995)

California Summer Case - Ozone

WRF Streamlines with Terrain Shaded
Nighttime: 1200UTC 01 Aug 2000

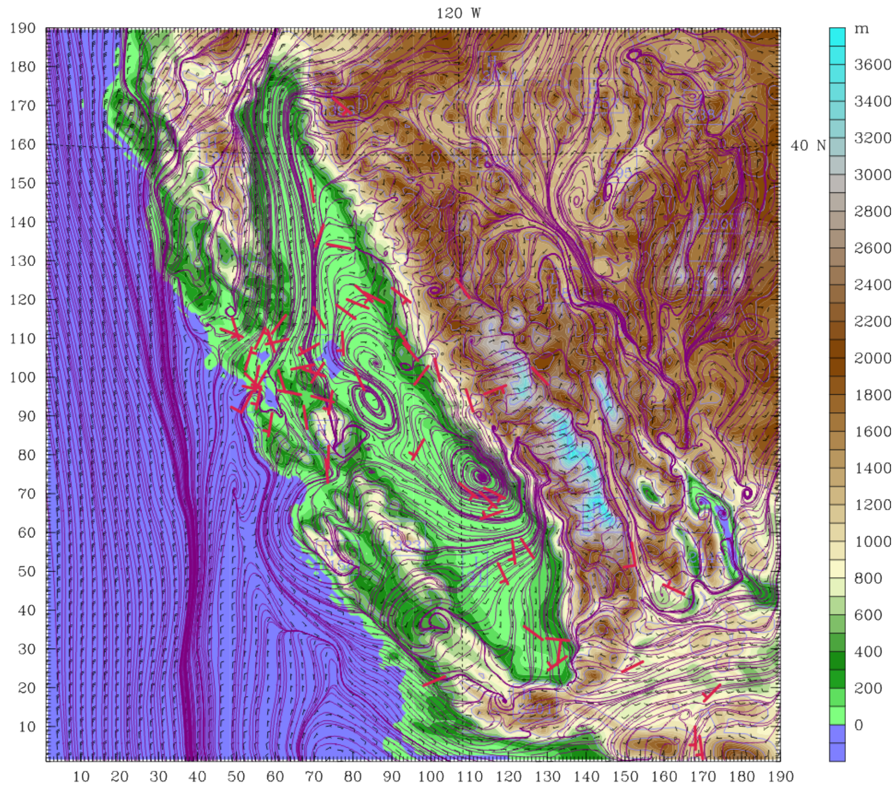

Multiscale FDDA – Analysis nudging on 36- and 12-km domains, obs nudging on 12- and 4-km domains

Schematic Diagram of Typical Regional Nighttime Flow

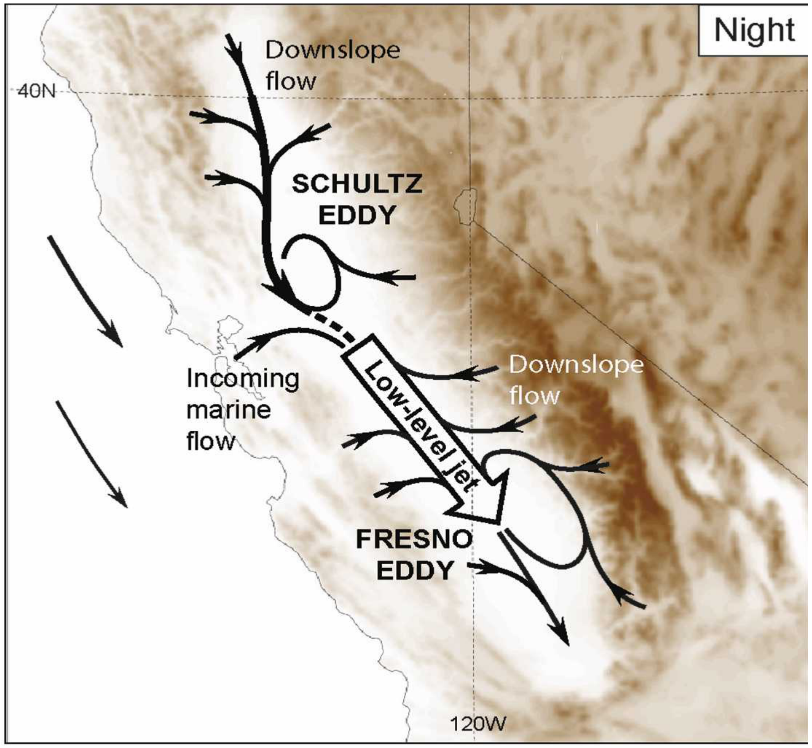

After Bao et al. (2008), Stauffer (1995)

Military-Defense:

U.S. Army MMS-Profiler Nowcast

AN/TMQ-52 MMS-Profiler Overview

smiths

- Provides MET support for artillery
  - Collect meteorological data from satellite, upper air radio soundings, and local surface conditions
  - Use meteorological data as input to weather forecast model to provide a snapshot of battlefield weather conditions
  - Communicate with fire support via tactical voice/ data radios.

Rapidly Relocatable Nowcast-Prediction System (RRNPS) for U.S. Army MMS-Profiler

- Comprised of MET sensors and a mesoscale modeling system running locally on the battlefield with continuous data assimilation to provide timely and accurate MET for use in correcting standard firing tables to accurately engage targets throughout the battlespace.

- Fielded to active Army units in early 2005, approved for full rate production in June 2005 with full 108-unit production cycle completed in 2010.

- Provides Local and Target Area ARTY MET messages every 15-30 minutes

- Provides as a minimum the MET Parameters
  - Temperature, Humidity, Pressure
  - Wind Speed, Wind Direction
  - Target Area: Ceiling, Visibility, Precip Rate, Precip Type

Army MMS-Profiler system with its crew, armed and wearing desert camouflage

PENNSTATE

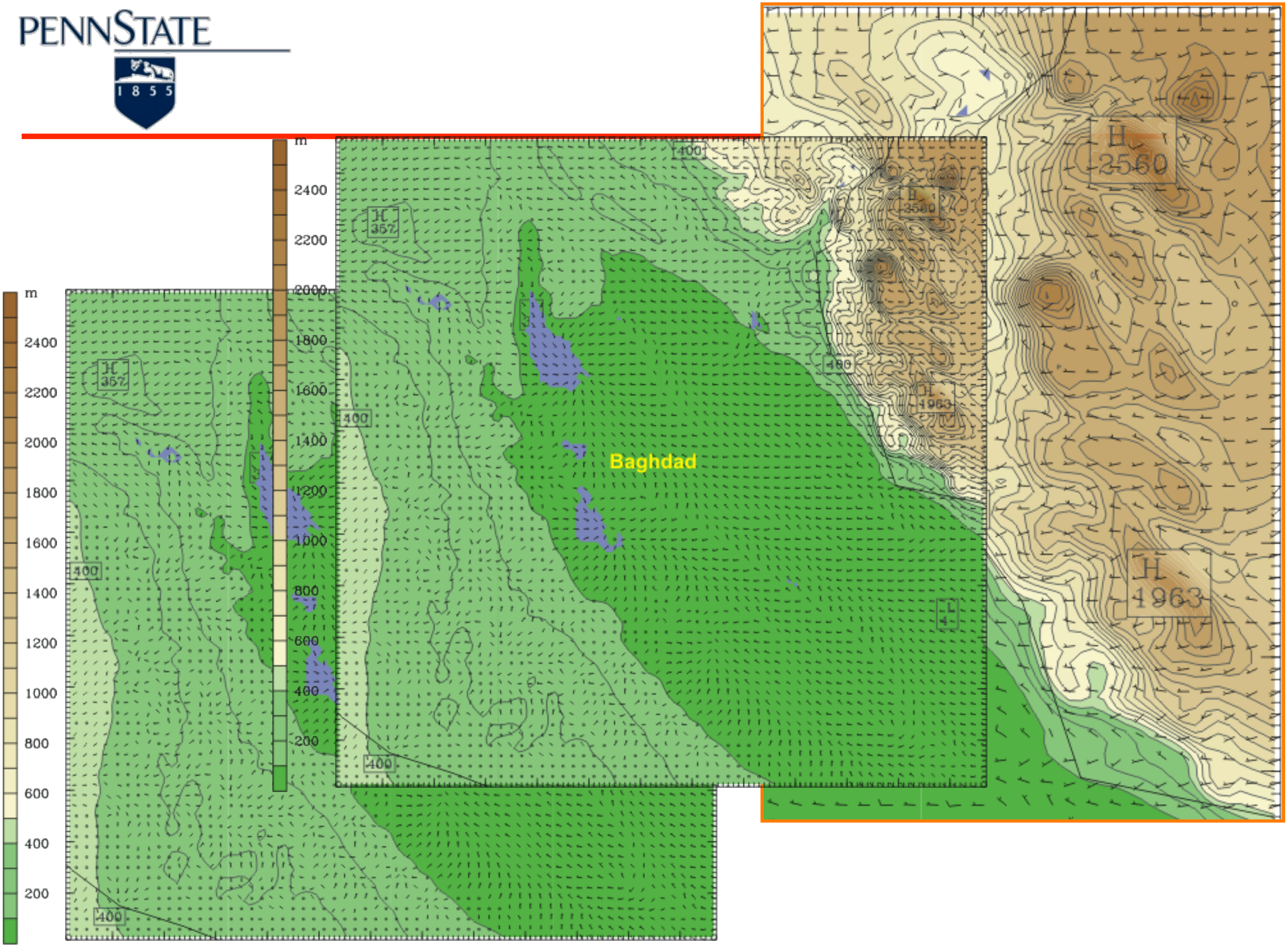

m
2400
2200
2000
1800
1600
1400
1200
1000
800
600
400
200
Baghdad
H
357
H
2560
H
1963
400

PENNSTATE

1855

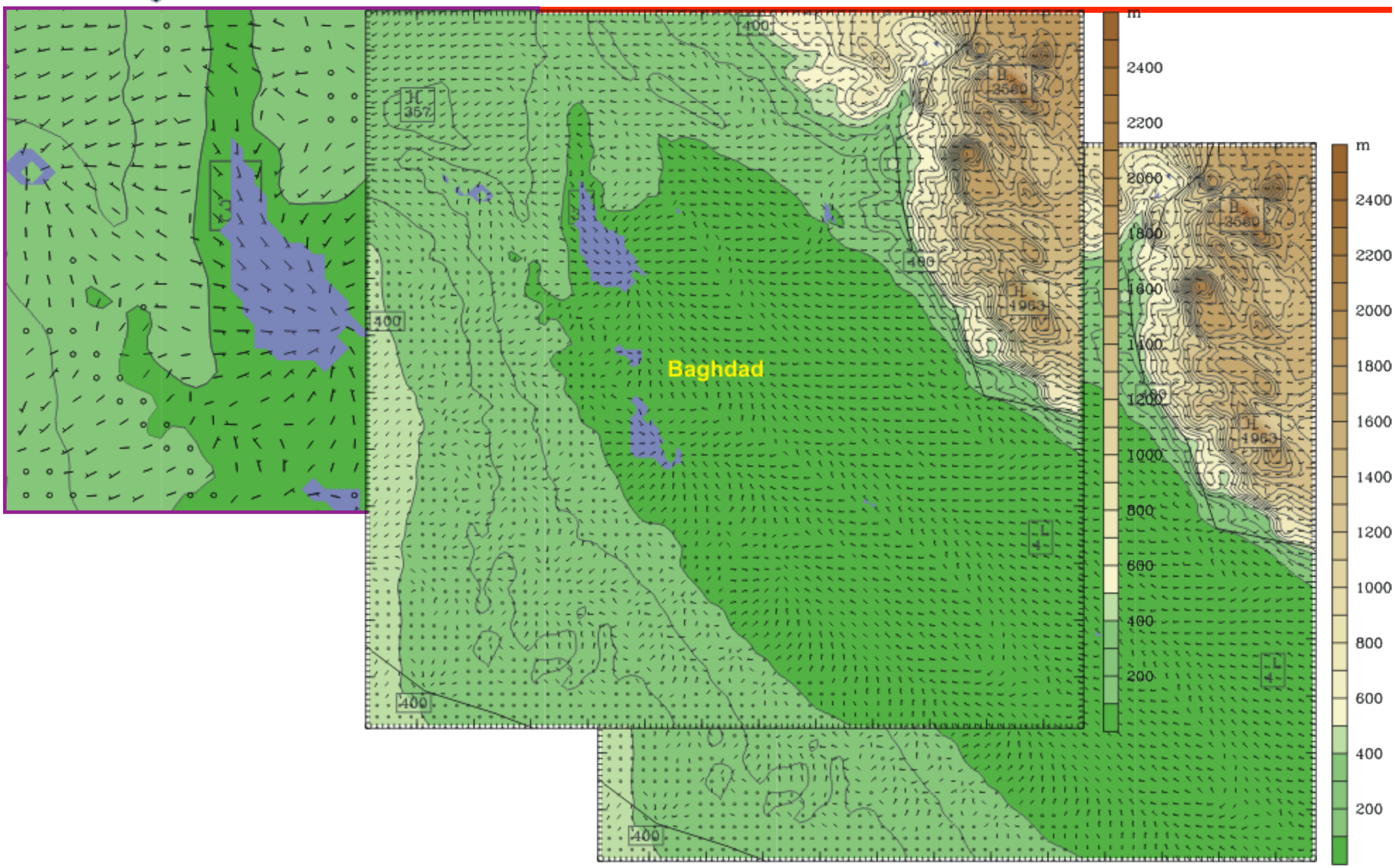

Military-Defense:

USMC METMF(R) NEXGEN

Meteorological Mobile Facility Replacement - Next Generation

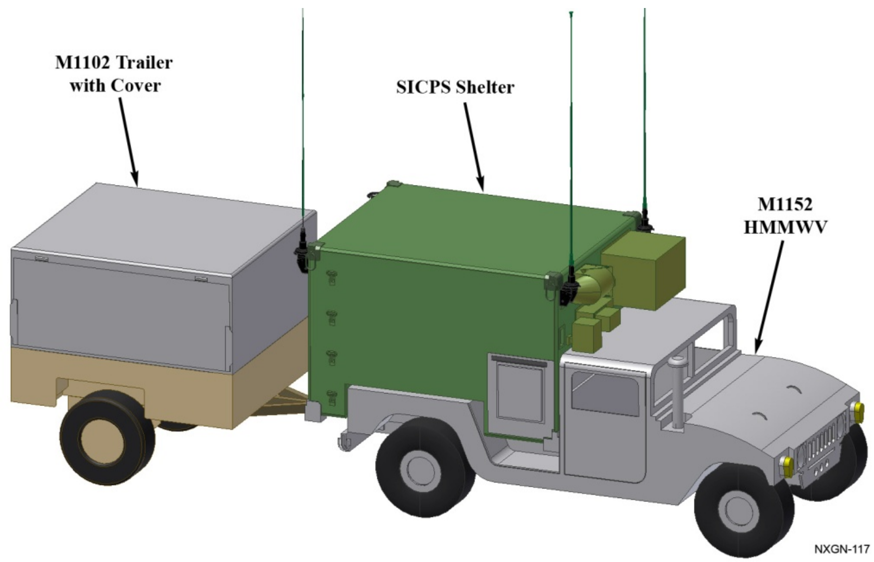

Military Defense: Defense Threat Reduction Agency (DTRA)

PENNSTATE

In-House Relocatable On-demand Forecast System (ROFS)

- Based on full-physics MM5/WRF
- Flexible or scheduled start and end times
- User-defined domains, sizes and horizontal/vertical resolutions
- Runs in real time and historical event modes
- Runs on massively parallel computing platforms (MPI)
- Continuous multi-scale four-dimensional data assimilation (FDDA) capability for improved model initialization (dynamic initialization)

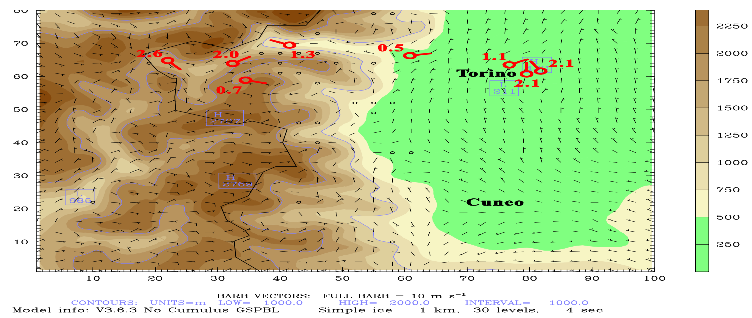

Torino Winter Olympics 2006

DTRA Connection article…

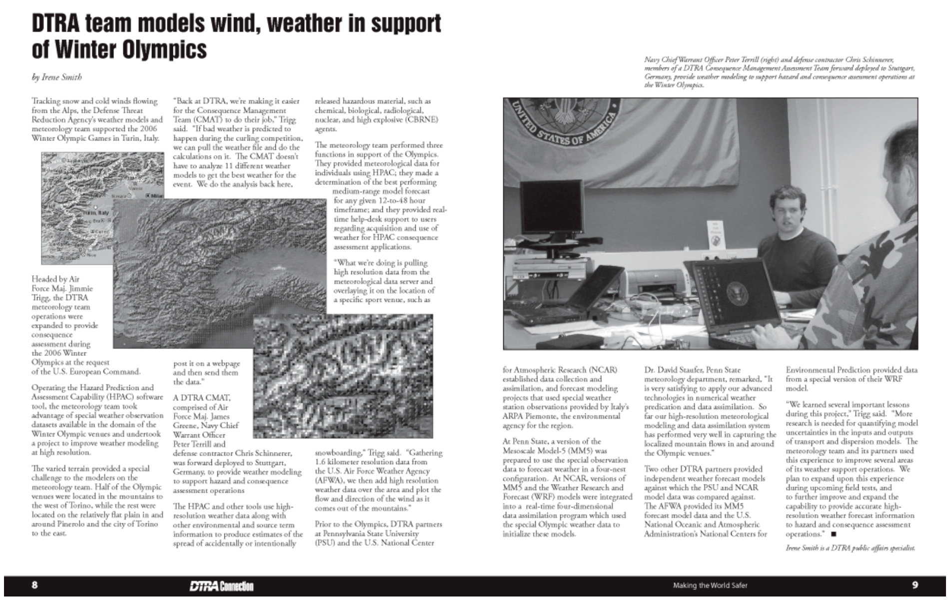

DTRA team models wind, weather in support of Winter Olympics

by Irene Smith

Tracking snow and cold winds flowing from the Alps, the Defense Threat Reduction Agency's weather models and meteorology team supported the 2006 Winter Olympic Games in Turin, Italy.

Headed by Air Force Maj. Jimmie Trigg, the DTRA meteorology team operations were expanded to provide consequence assessment during the 2006 Winter Olympics at the request of the U.S. European Command.

Operating the Hazard Prediction and Assessment Capability (HPAC) software tool, the meteorology team took advantage of special weather observation datasets available in the domain of the Winter Olympic venues and undertook a project to improve weather modeling at high resolution.

The varied terrain provided a special challenge to the modelers on the meteorology team. Half of the Olympic venues were located in the mountains to the west of Torino, while the rest were located on the relatively flat plain in and around Pinerolo and the city of Torino to the east.

"Back at DTRA, we're making it easier for the Consequence Management Team (CMAT) to do their job," Trigg said. "If bad weather is predicted to happen during the curling competition, we can pull the weather file and do the calculations on it. The CMAT doesn't have to analyze 11 different weather models to get the best weather for the event. We do the analysis back here, post it on a webpage and then send them the data."

A DTRA CMAT, comprised of Air Force Maj. James Greene, Navy Chief Warrant Officer Peter Terrill and defense contractor Chris Schinnerer, was forward deployed to Stuttgart, Germany, to provide weather modeling to support hazard and consequence assessment operations

The HPAC and other tools use high-resolution weather data along with other environmental and source term information to produce estimates of the spread of accidentally or intentionally released hazardous material, such as chemical, biological, radiological, nuclear, and high explosive (CBRNE) agents.

The meteorology team performed three functions in support of the Olympics. They provided meteorological data for individuals using HPAC; they made a determination of the best performing medium-range model forecast for any given 12-to-48 hour timeframe; and they provided real-time help-desk support to users regarding acquisition and use of weather for HPAC consequence assessment applications.

"What we're doing is pulling high resolution data from the meteorological data server and overlaying it on the location of a specific sport venue, such as snowboarding," Trigg said. "Gathering 1.6 kilometer resolution data from the U.S. Air Force Weather Agency (AFWA), we then add high resolution weather data over the area and plot the flow and direction of the wind as it comes out of the mountains."

Prior to the Olympics, DTRA partners at Pennsylvania State University (PSU) and the U.S. National Center for Atmospheric Research (NCAR) established data collection and assimilation, and forecast modeling projects that used special weather station observations provided by Italy's ARPA Piemonte, the environmental agency for the region.

At Penn State, a version of the Mesoscale Model-5 (MM5) was prepared to use the special observation data to forecast weather in a four-nest configuration. At NCAR, versions of MM5 and the Weather Research and Forecast (WRF) models were integrated into a real-time four-dimensional data assimilation program which used the special Olympic weather data to initialize these models.

Dr. David Staufer, Penn State meteorology department, remarked, "It is very satisfying to apply our advanced technologies in numerical weather predication and data assimilation. So far our high-resolution meteorological modeling and data assimilation system has performed very well in capturing the localized mountain flows in and around the Olympic venues."

Two other DTRA partners provided independent weather forecast models against which the PSU and NCAR model data was compared against. The AFWA provided its MM5 forecast model data and the U.S. National Oceanic and Atmospheric Administration's National Centers for Environmental Prediction provided data from a special version of their WRF model.

"We learned several important lessons during this project," Trigg said. "More research is needed for quantifying model uncertainties in the inputs and outputs of transport and dispersion models. The meteorology team and its partners used this experience to improve several areas of its weather support operations. We plan to expand upon this experience during upcoming field tests, and to further improve and expand the capability to provide accurate high-resolution weather forecast information to hazard and consequence assessment operations." ■

Irene Smith is a DTRA public affairs specialist.

Navy Chief Warrant Officer Peter Terrill (right) and defense contractor Chris Schinnerer, members of a DTRA Consequence Management Assessment Team forward deployed to Stuttgart, Germany, provide weather modeling to support hazard and consequence assessment operations at the Winter Olympics.

8 DTRA Connection — Making the World Safer 9

PSU 1.3km ROFS winds (Feb. 22/14 UTC) and HPAC/SCIPUFF predictions (Feb. 22/13-17 UTC)

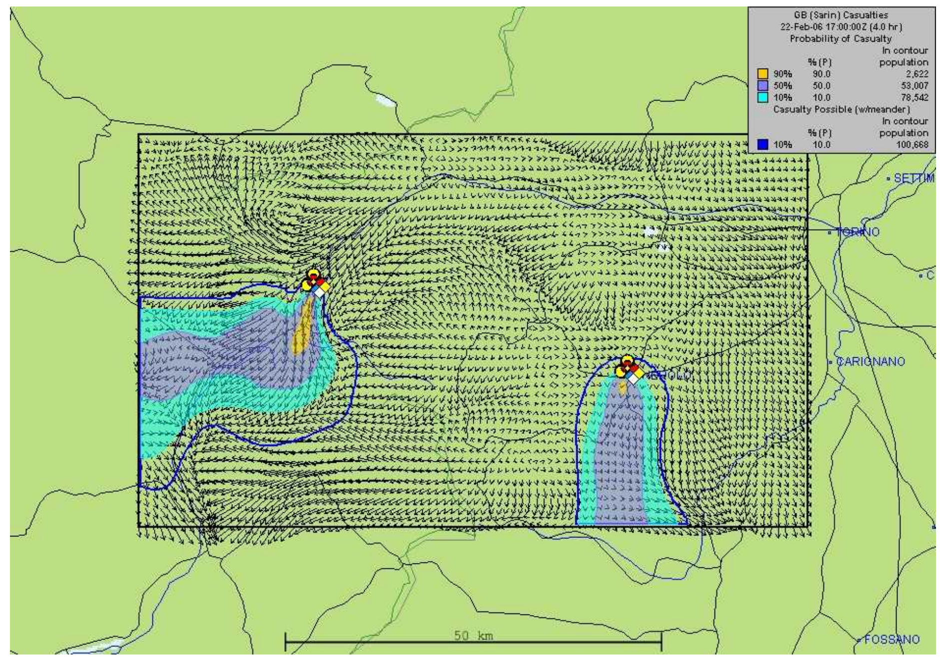

Super Bowl XLI 2007

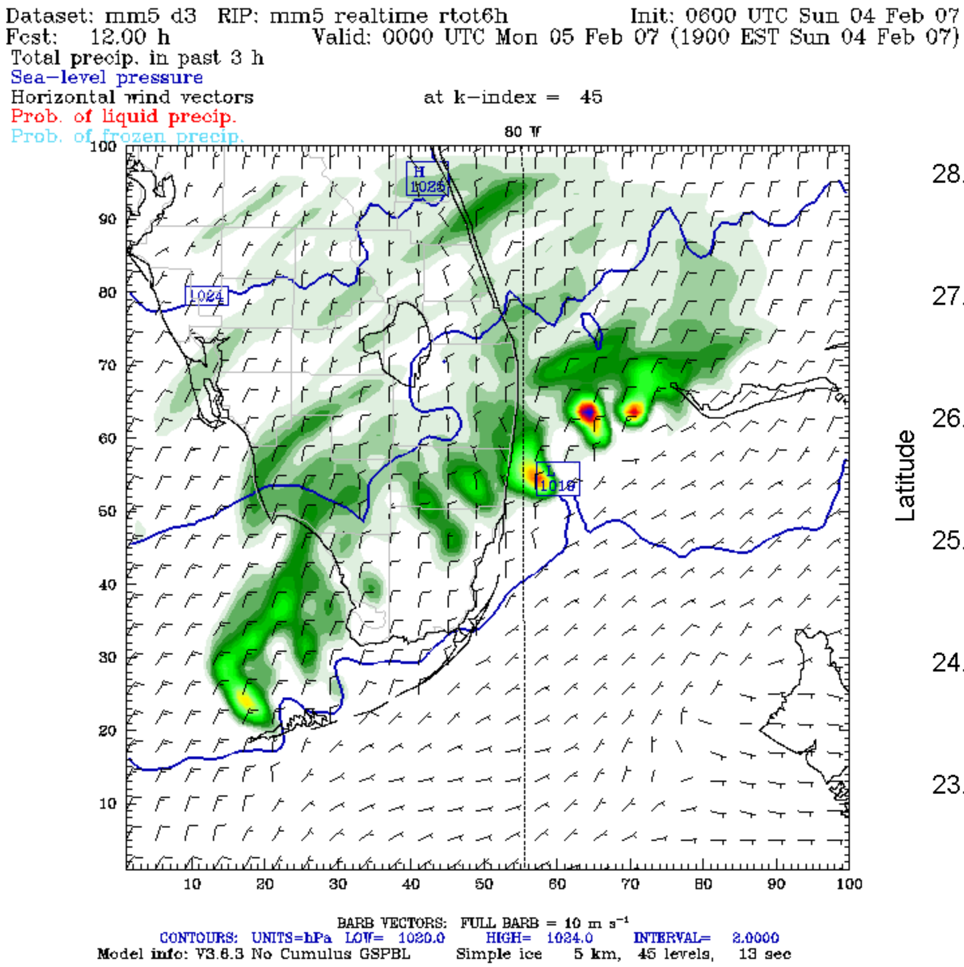

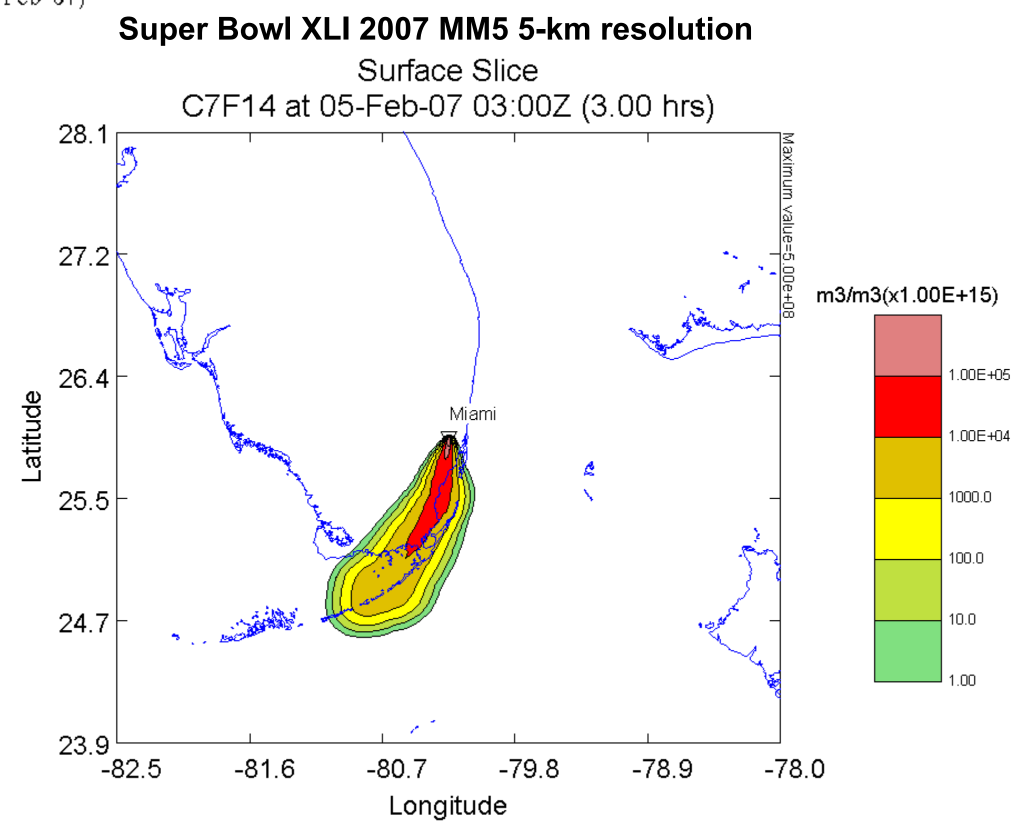

Beijing Summer Olympics 2008

Chine s at
06 UT t

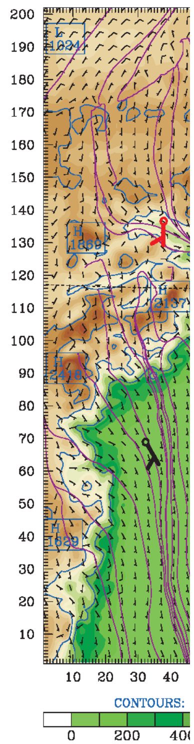

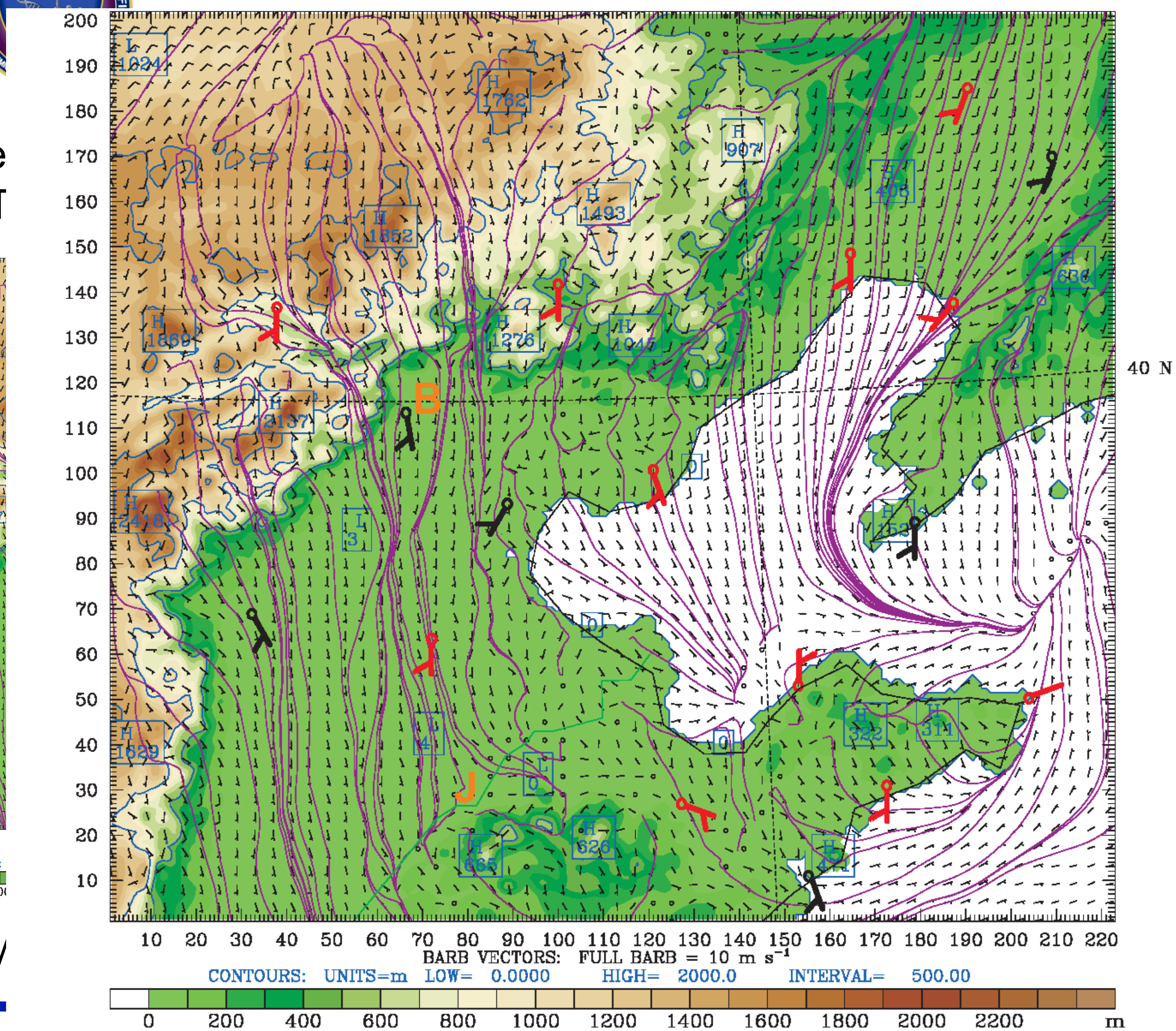

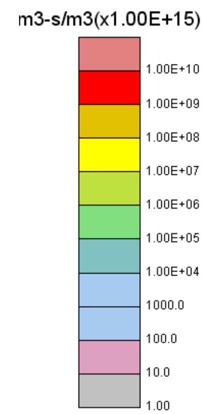

l

Black=WM

UNCLASSIFIED

Denver Democratic National Convention 2008

PENNSTATE

The use of a 1.3
domain allowed
accurate foreca
surface wind
confluence line
UTC (2000 LST
the front range
Rockies.

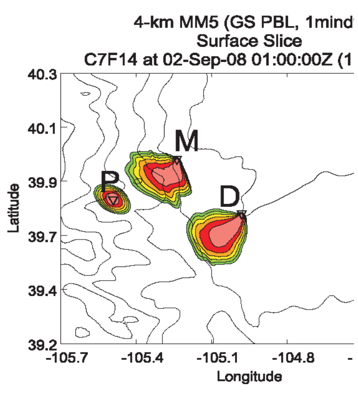

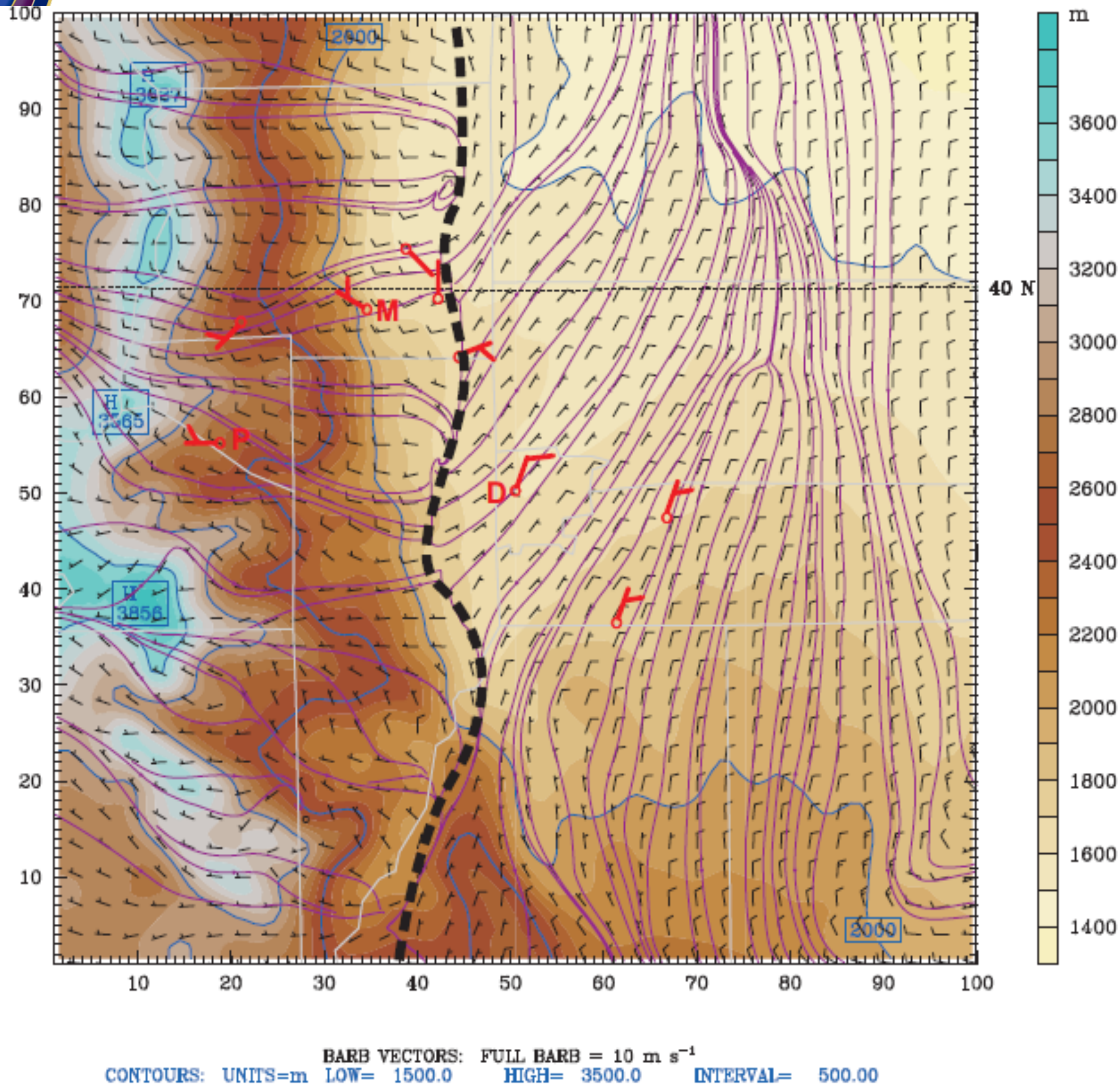

e line,
westerly
w to the
erly large
ne east,
plumes

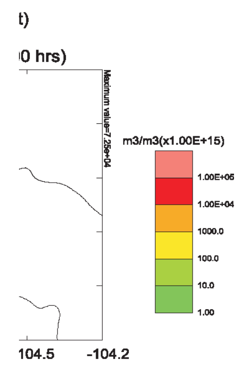

PENNSTATE

Vancouver Winter Olympics 2010

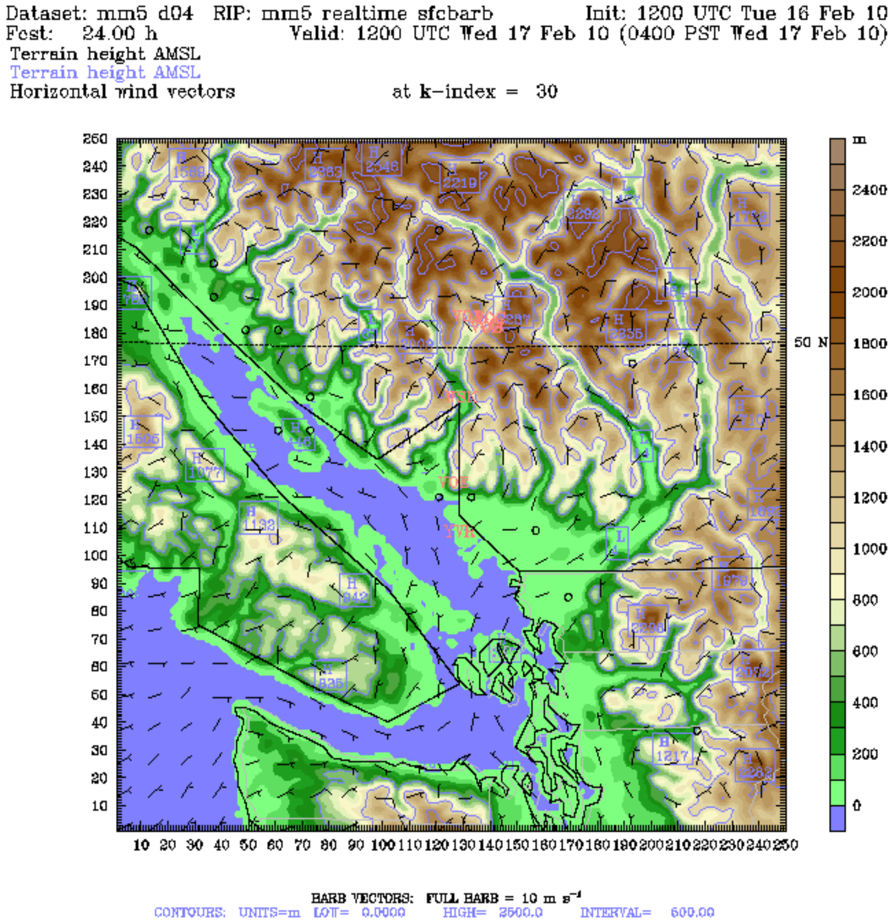

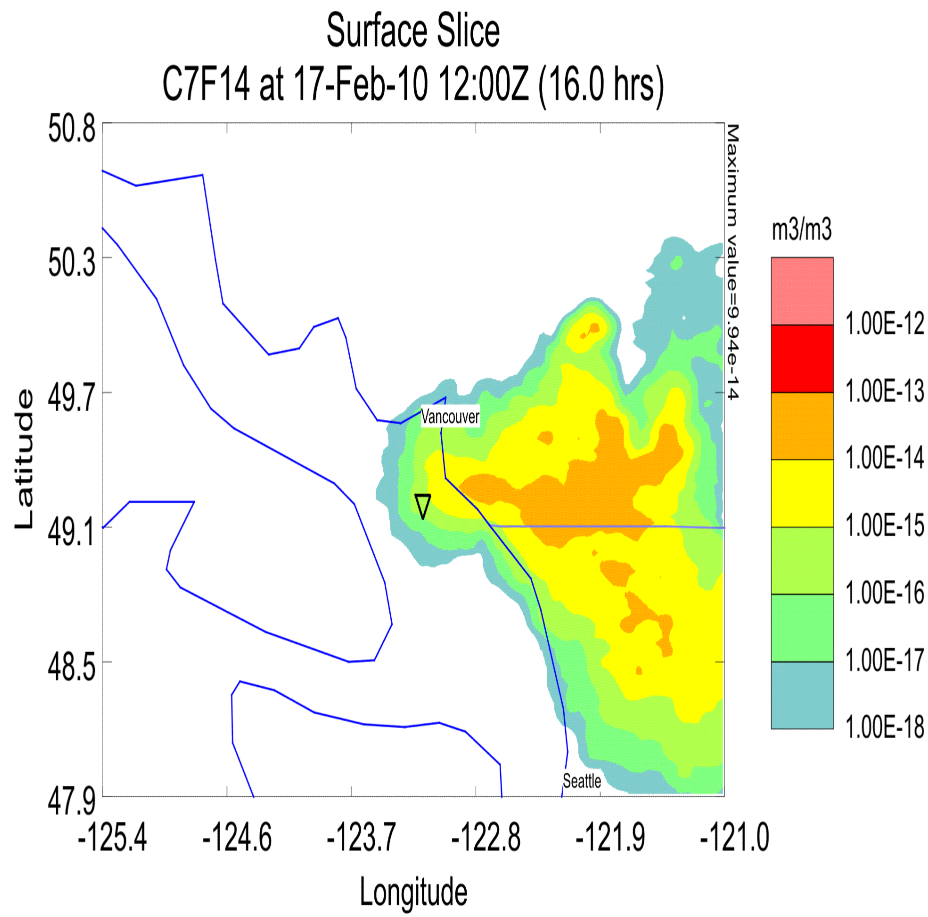

PENNSTATE

Fukushima 2011

36 km

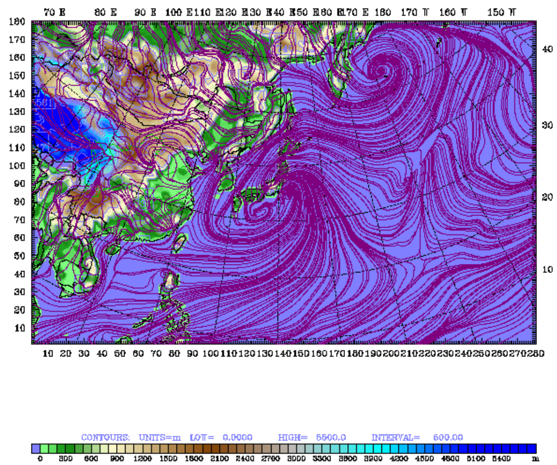

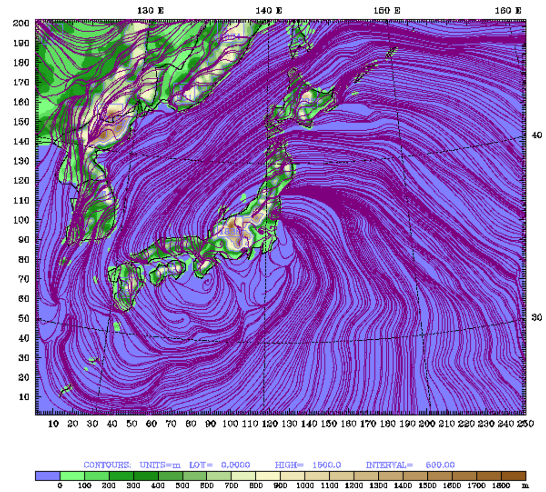

12 km

PSU / DTRA Reachback Forensic Analysis of Fukushima

4 km

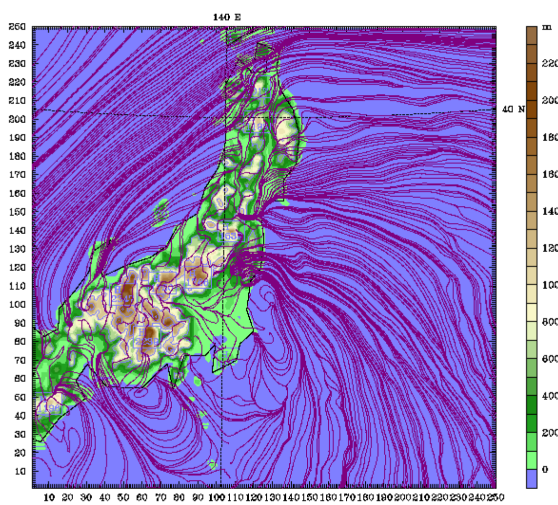

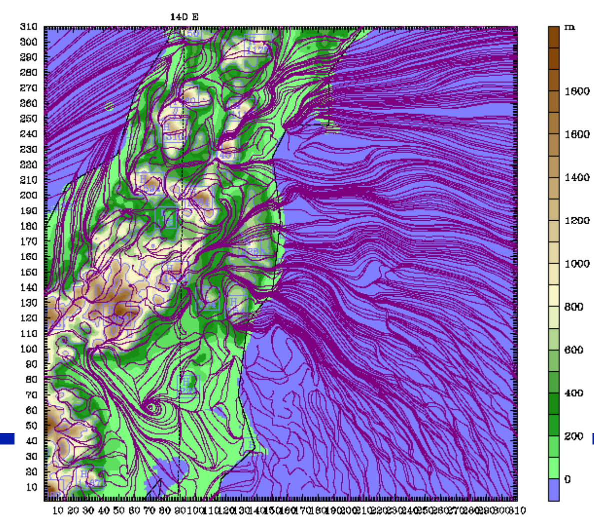

1.3 km

Aviation:

Interim Progress Report
on
A NextGen Airport Forecast System (NGAFS)

Cooperative Agreement
between
NOAA/NWS/OST and Penn State Univ.

Silver Spring, MD
20 July 2011

David R. Stauffer, P.I., PSU

NGAFS Motivation

Objective: Build, test and evaluate a local-data assimilating, high-resolution numerical / statistical airport forecast system to dynamically downscale operational numerical products, yielding more detailed and accurate aviation forecast parameters.

Cooperative Approach

- **Penn State will build a numerical modeling system with overall characteristics similar to the experimental HRRR model under development at NOAA/OAR/GSD.**
  - ARW dynamical core; RUC-like physics.
  - ICs and LBCs from RR; RUC LSM at lower boundary.
  - 1-h cycling of 6-h to 12-h forecasts.
  - Partial-cycling data assimilation of local observations.
  - Highest grid resolution ~ 1 km.

- **NOAA/NWS/OST/MDL will use Penn State ARW products as an input to a LAMP-like system to forecast aviation-sensitive Wx parameters in the vicinity of major airports.**
  - Hourly observations and analyses.
  - *GFS/LAMP-based MOS updated with PSU ARW 1-km forecasts.*

PSU Realtime Systems

- Central PA Centered WRF
  - http://www.meteo.psu.edu/~wrfrt/
- NGAFS WRF
  - http://www.meteo.psu.edu/~ngafs/
- Stable Boundary Layer WRF
  - http://www.meteo.psu.edu/~wrfrt1/

create
collaborate
communicate

Basic Research:

July 2011

Improved Understanding and Prediction of the Stable Boundary Layer to Better Predict the Fate of Airborne Toxics Released by WMDs HDTRA1-10-0033

DEFENSE THREAT REDUCTION AGENCY JOINT SCIENCE AND TECHNOLOGY OFFICE CHEMICAL AND BIOLOGICAL DEFENSE

David R. Stauffer, PI
Professor, Penn State University
Defense Threat Reduction Agency (DTRA)

Project Objective

- To understand and predict the structure and variability of stable boundary layers (SBLs) to improve predictions of atmospheric transport and dispersion (AT&D) of airborne toxic materials from accidents or WMDs.

PENNSTATE

Combined modeling and observation study

WRF smallest domain (0.444 km horizontal resolution)

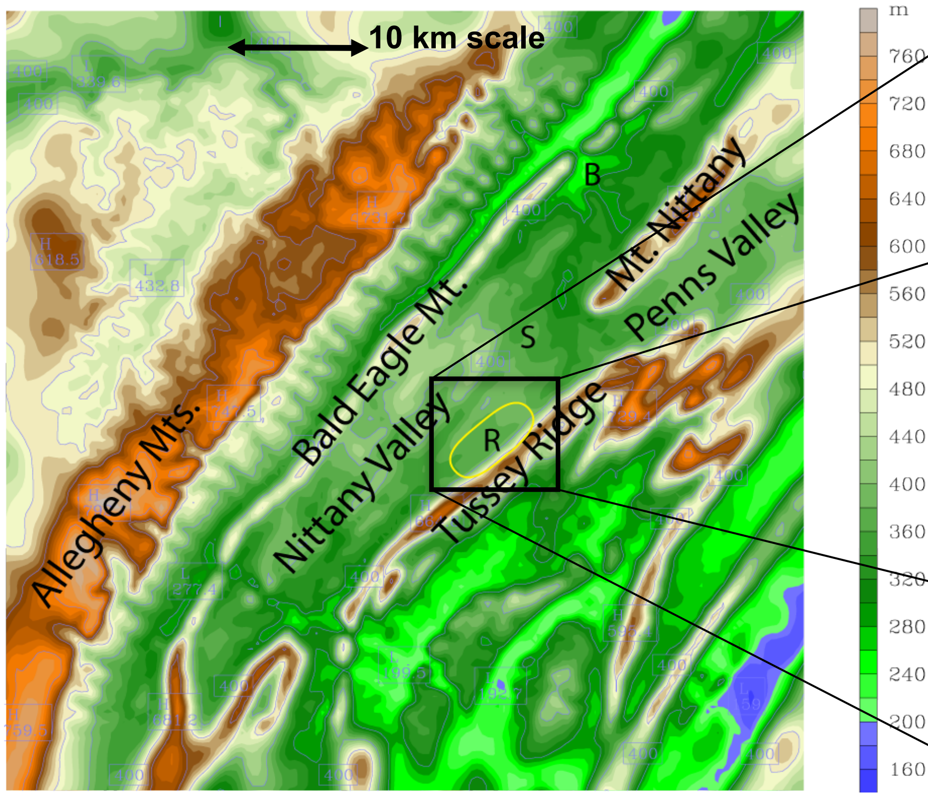

Observation Network

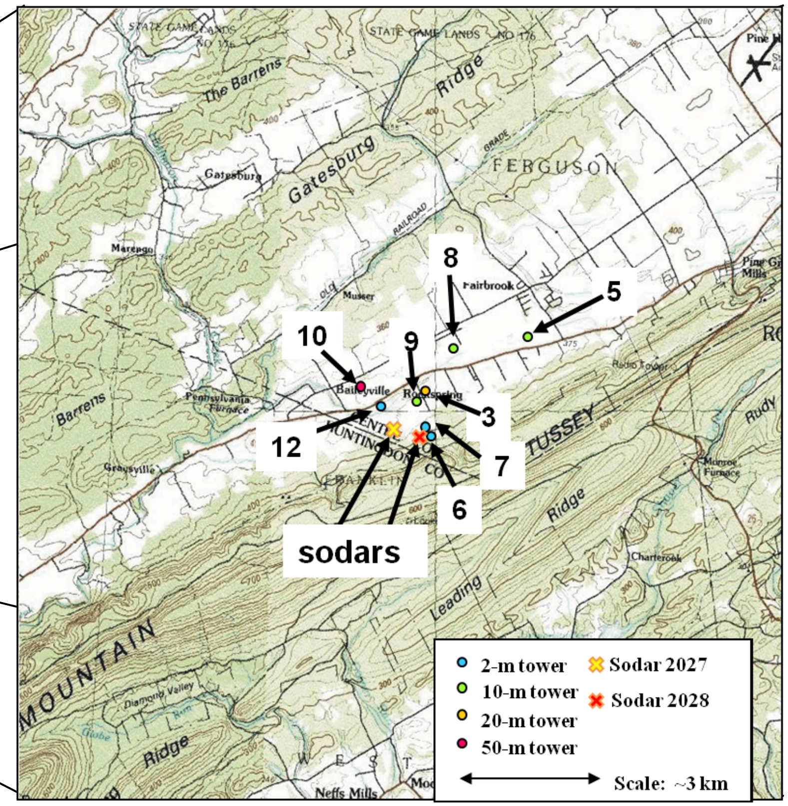

WRF-ARW Model Configuration

- WRF uses nested domains with 12-, 4-, 1.33, and 0.44-km horizontal grid spacing. Sub-kilometer horizontal resolution to resolve fine-scale terrain important for shallow SBL flows and AT&D.

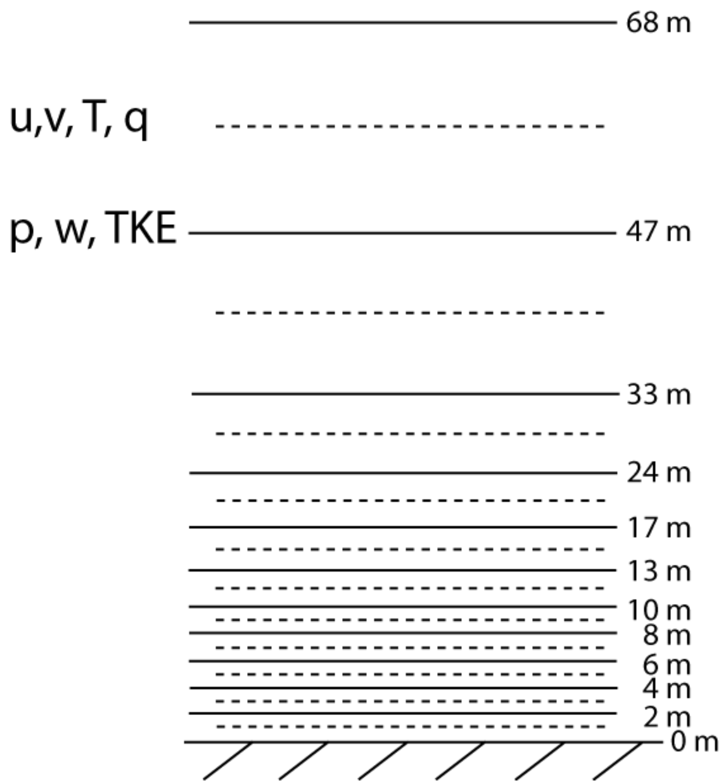

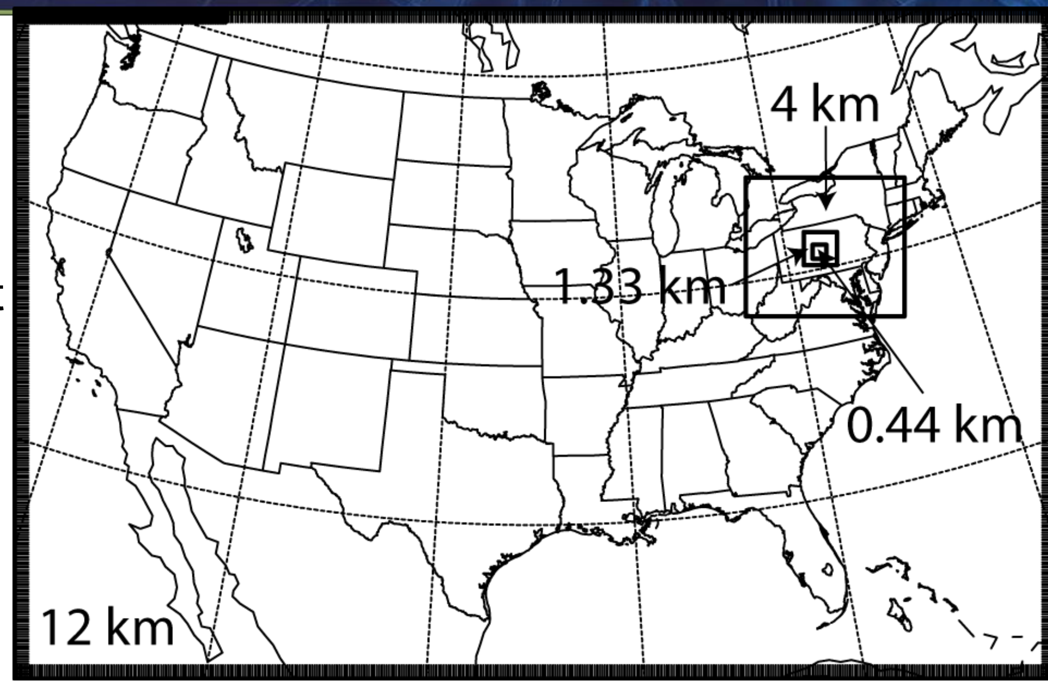

- Very high vertical resolution near the surface to resolve shallow SBL and gravity-driven slope flows (10 layers in lowest 50 m AGL).
- 12-hour forecasts from 00 to 12 UTC (7PM to 7AM EST)
- Model output, saved every 12 minutes, is used to represent submeso fluctuations in trajectories and AT&D predictions

WRF MYJMod PBL Physics Model and Observed Surface Winds

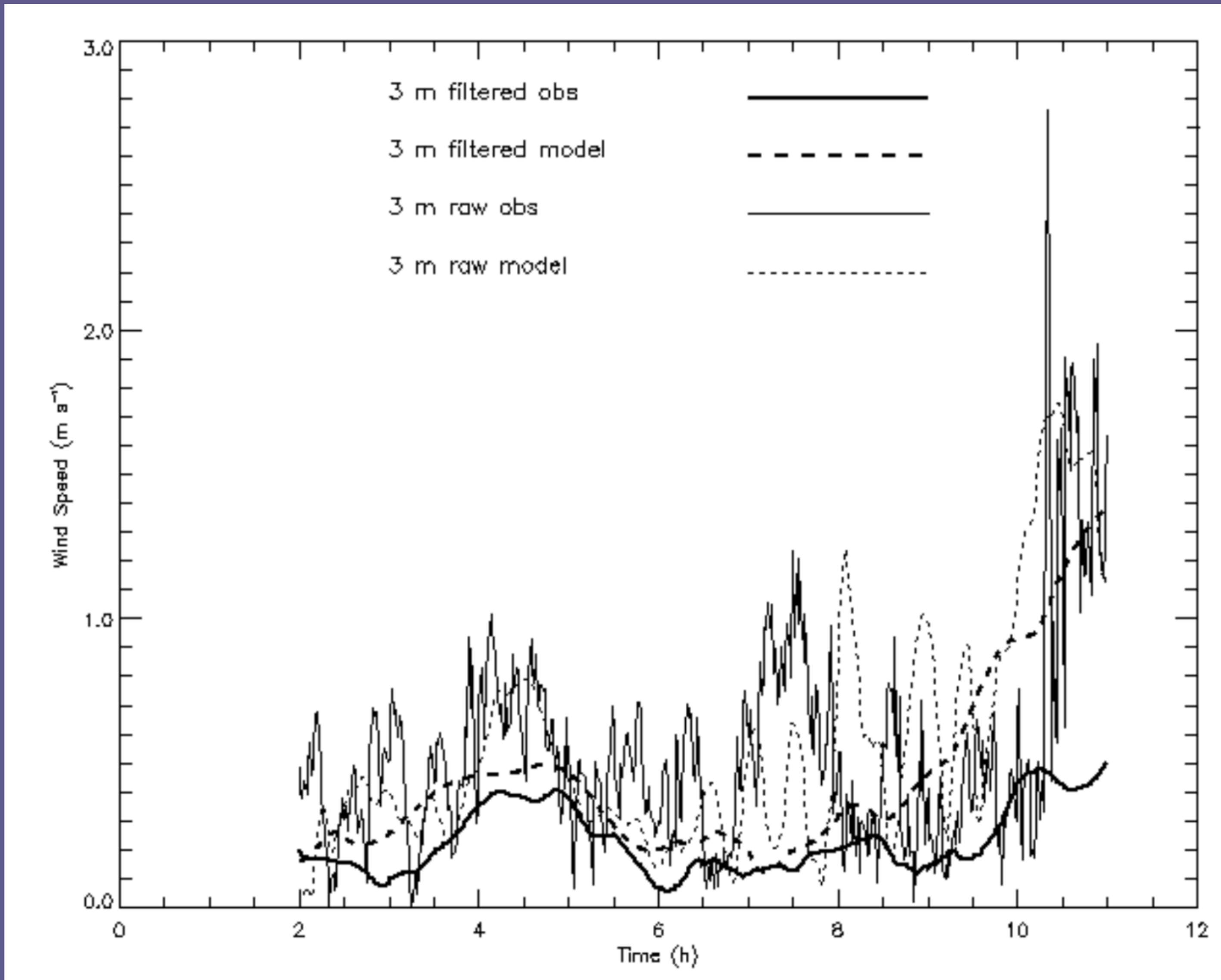

Conceptual Model of Nocturnal Flow Regimes For Valleys with Weak Down-valley Terrain Slopes

Internal waves and other submeso motions cause intermittent turbulence near the surface

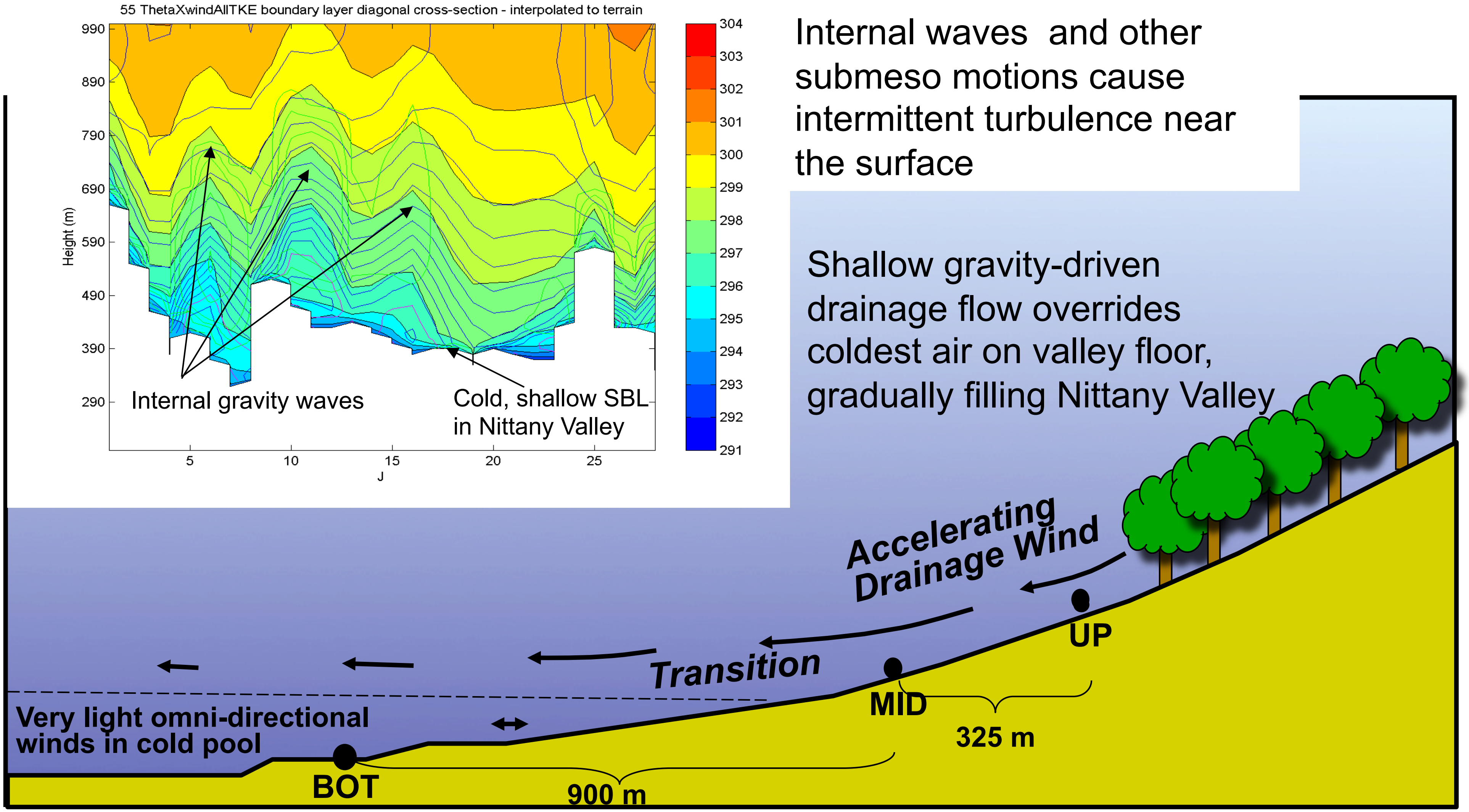

Shallow gravity-driven drainage flow overrides coldest air on valley floor, gradually filling Nittany Valley

Wave structures are captured by the observing network (Josh Hoover, Scott Richardson)

Wave-like pattern in wind speed and vertical motion

Sodar

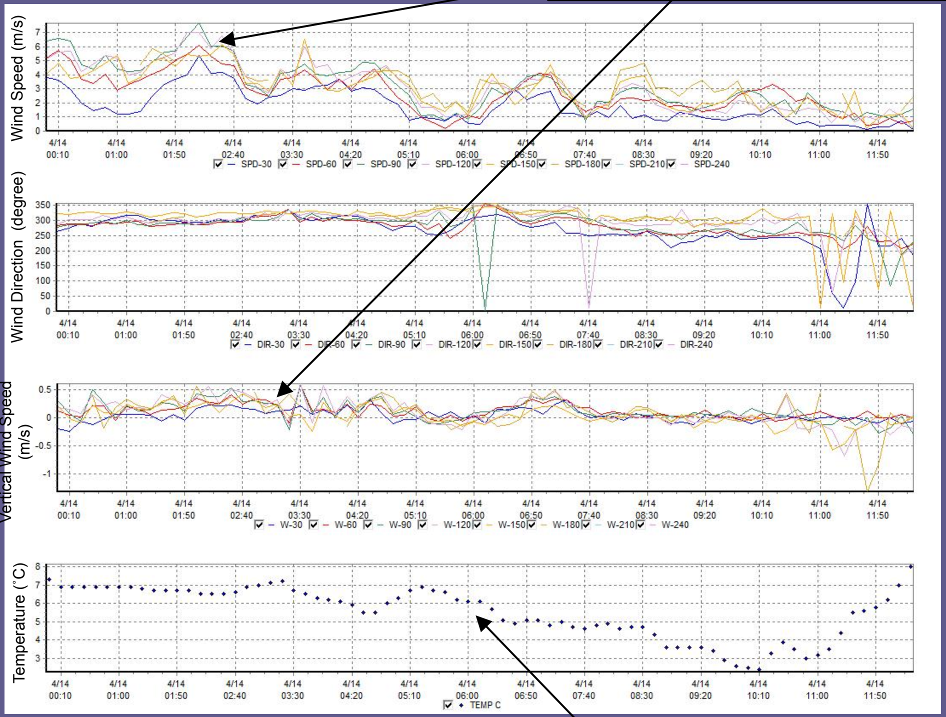

Tower Temperature (C) located at Site 9

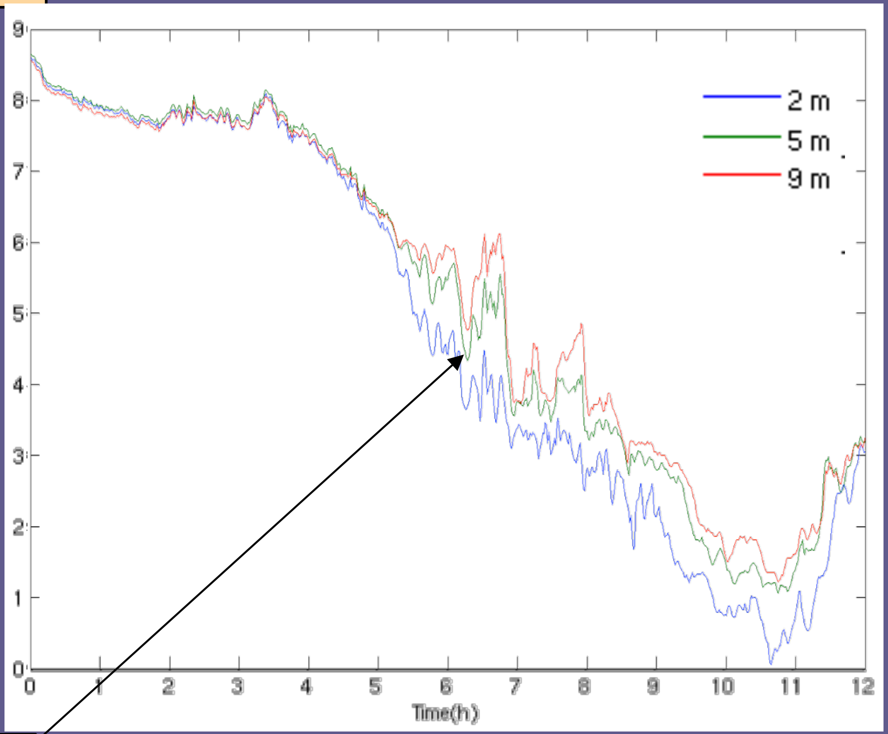

Periodic fluctuations of 3-m temperature over several hours

Effect of Internal Gravity Waves on the Stable Boundary Layer (SBL) (Astrid Suarez, Brian Reen)

Positive temperature fluctuation is associated with the passage of the wave crest and the underlying rotor. As the wave propagates upstream, the rotor-induced circulation causes the surface cold pool to erode between 0600-0630 UTC and brings higher potential temperature air to the surface.

a)Observed Site 9 1-min Averaged Tower Data

b) Modeled Site 9 1-min Instantaneous Output

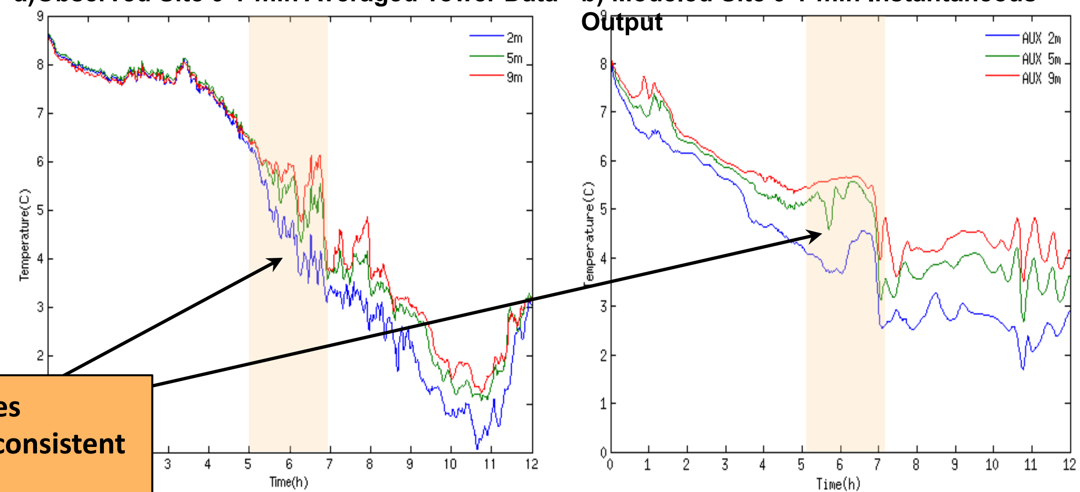

WRF model produces structures that are consistent with observations

★ Location of Site 9

a) 0536 UTC

b) 0600 UTC

c) 0624 UTC

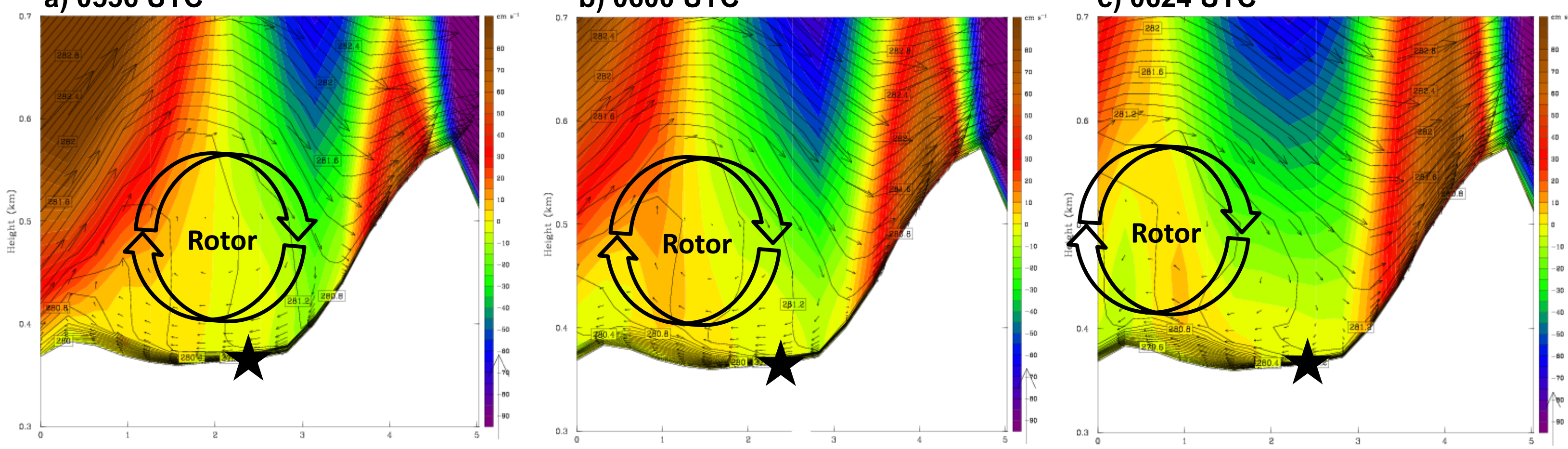

Vertical Velocity

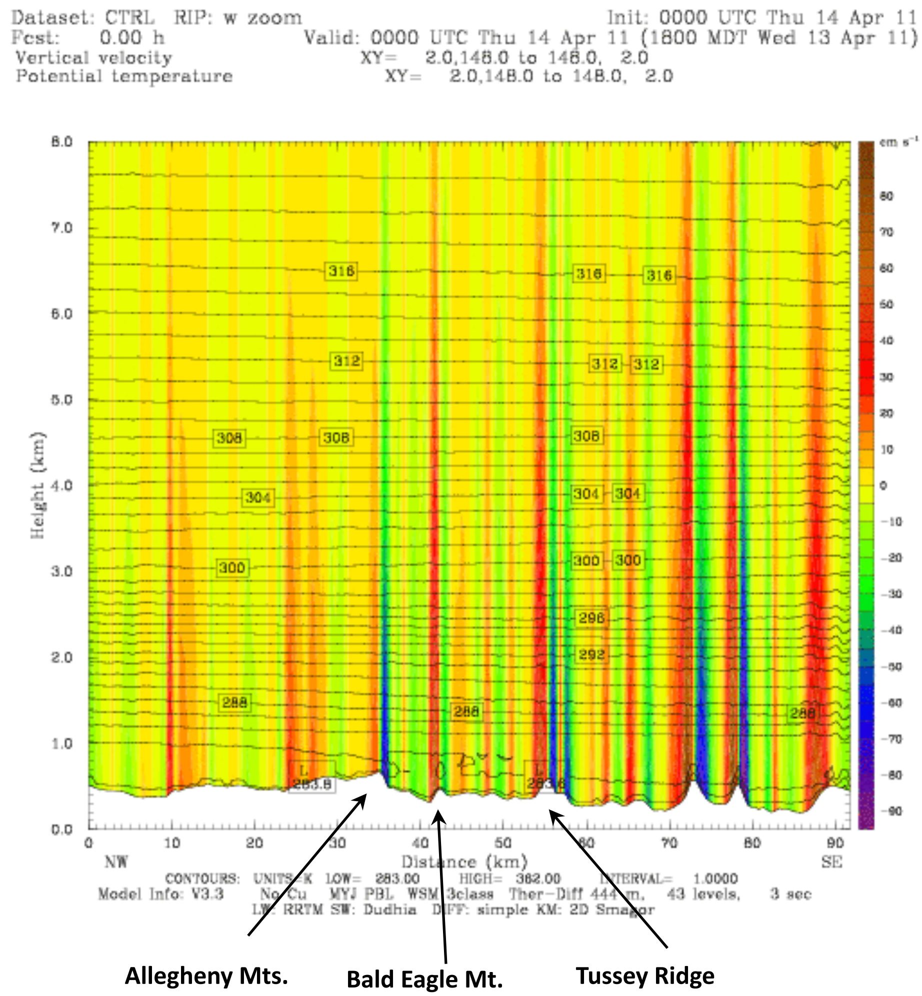

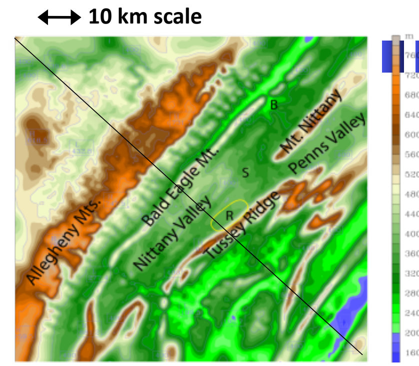

Hovmoller Diagram for Vertical Motion

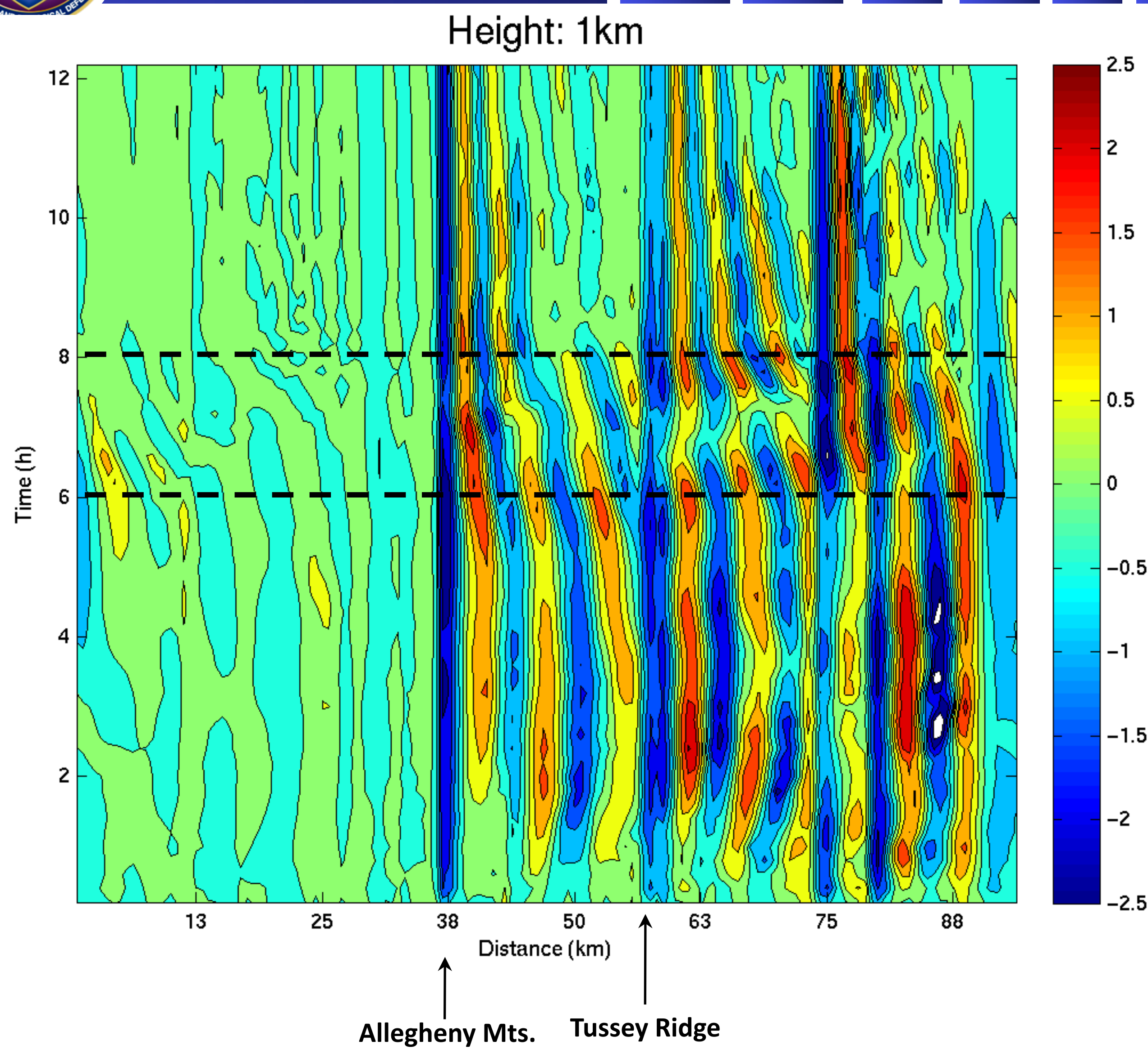

5-m Releases at Site 9

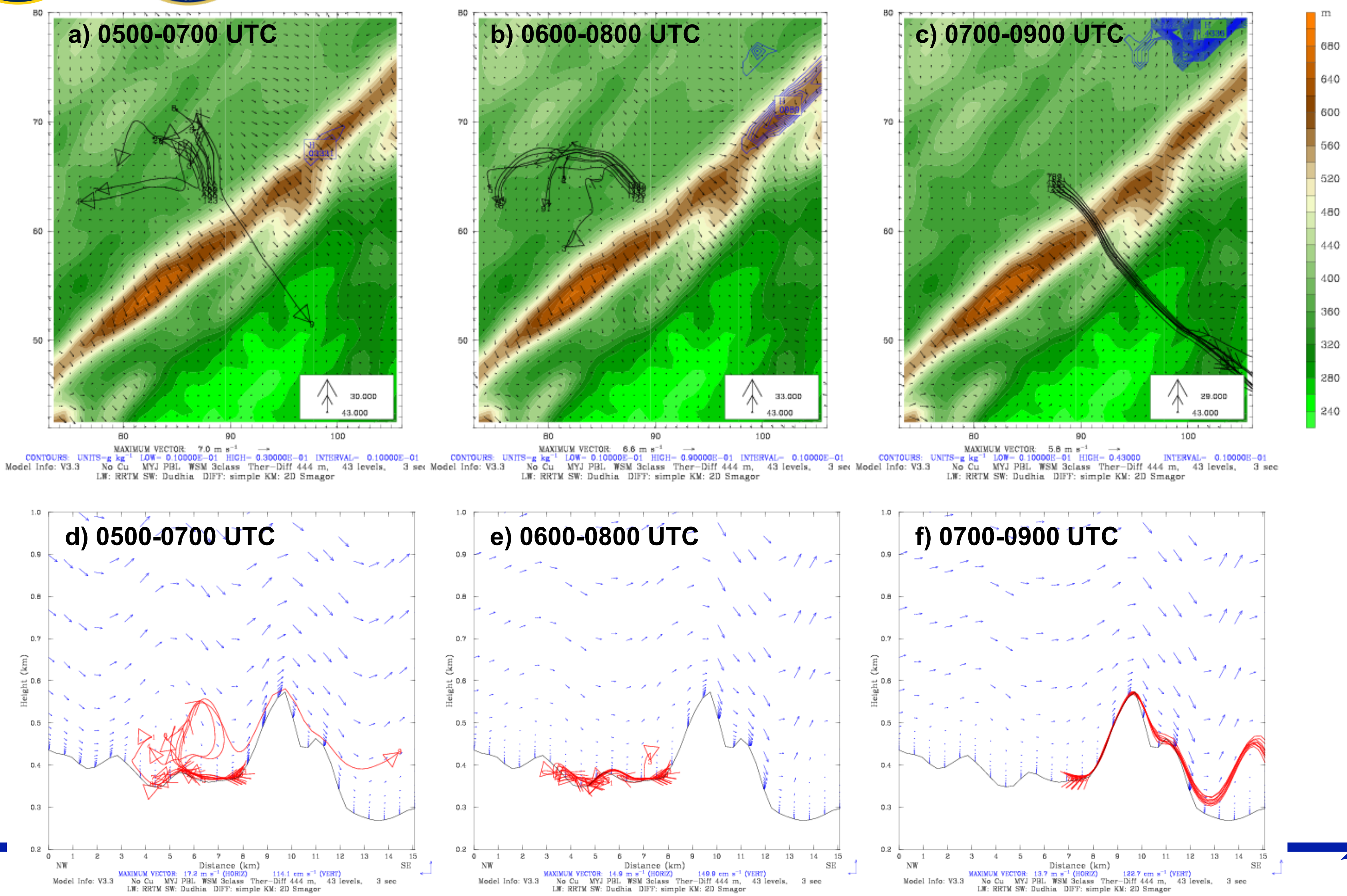

SCIPUFF Surface Dosage and Concentration of 5-m Release at Site 9

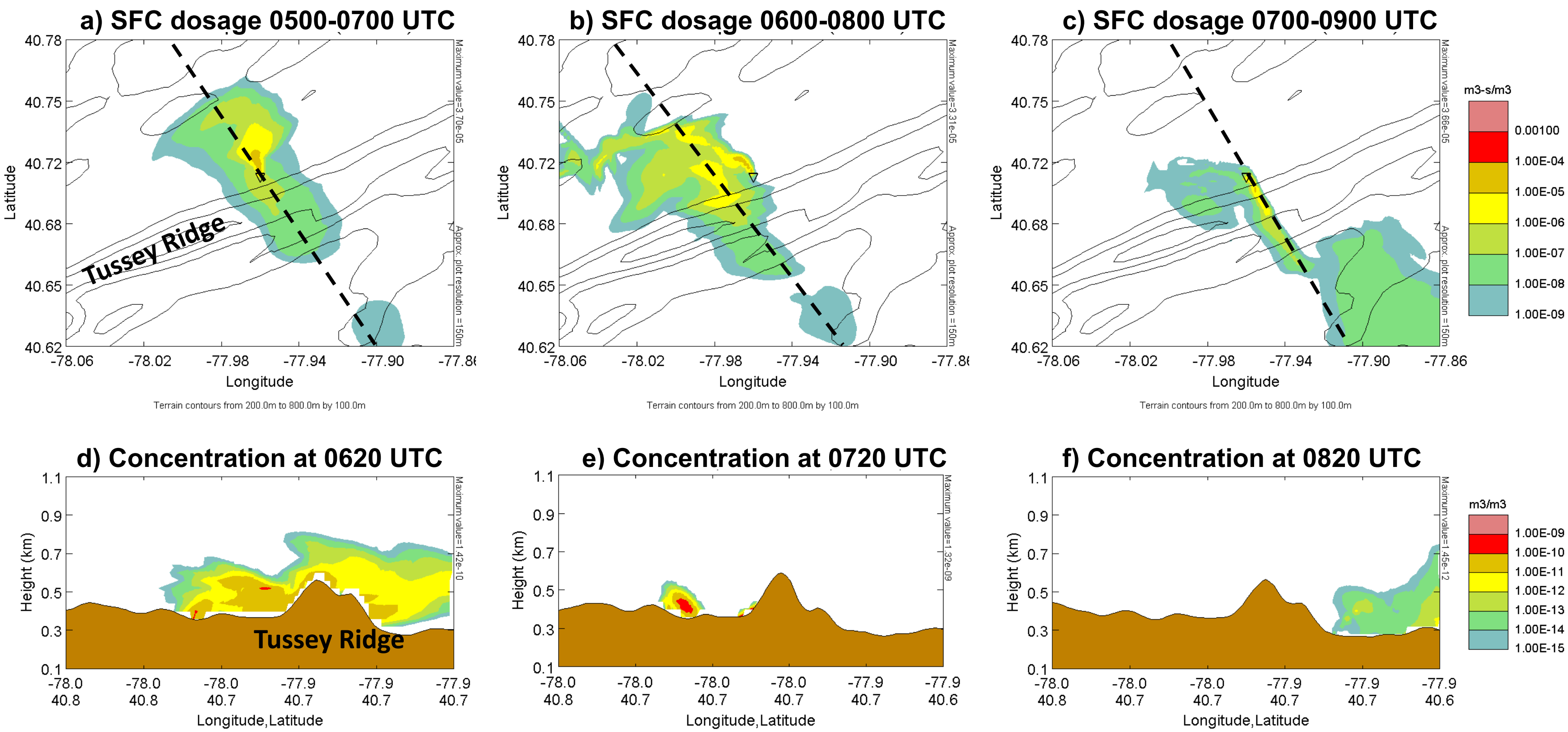

PENNSTATE

Effect of Internal Gravity Waves on Hazard Prediction

a) Trajectories from 0500-0700 UTC

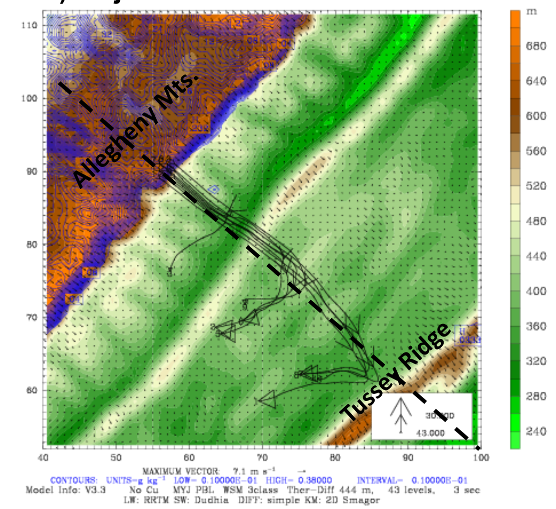

b) Surface Dosage at 0700 UTC

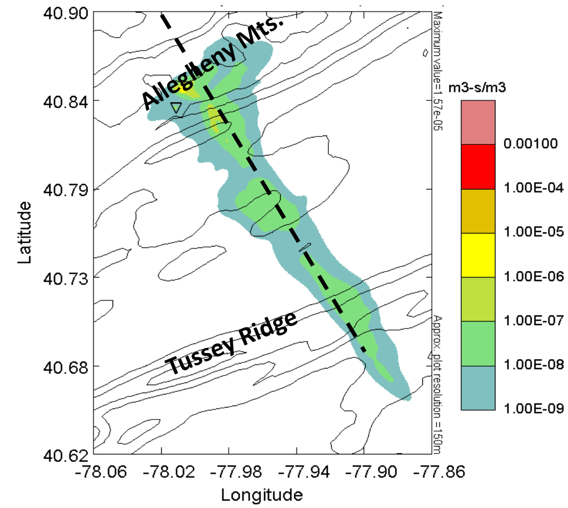

c) Trajectories from 0500-0700 UTC

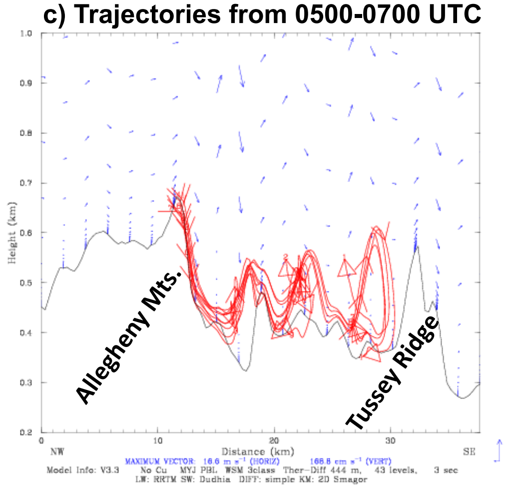

d) Cross-section of concentration at 0700 UTC

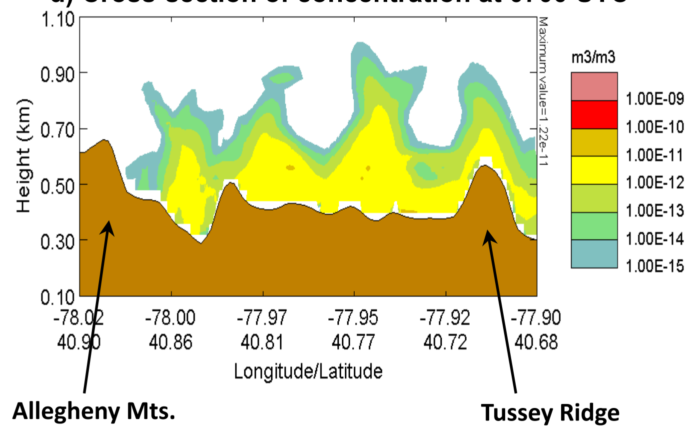

Terrain-induced gravity waves were found to have an impact on AT&D.

- **Small changes in the location of the wave crest and underlying rotor result in significantly different transport and dispersion patterns.**
- **Rotors can also transport harmful materials suspended above ground level to the surface or circulate surface releases over the same location.**
- **Terrain-induced gravity waves can also affect the downstream transport of harmful materials.**

Additional cases are needed in order to test the sensitivity of AT&D to the presence of internal-gravity waves and the ability of the model to forecast non-wave cases versus stationary and non-stationary wave events. More R&D is also needed to improve the model physics for these weak wind, stable conditions.

Ensembles: Advanced Data Assimilation (Lili Lei)

Nudging:

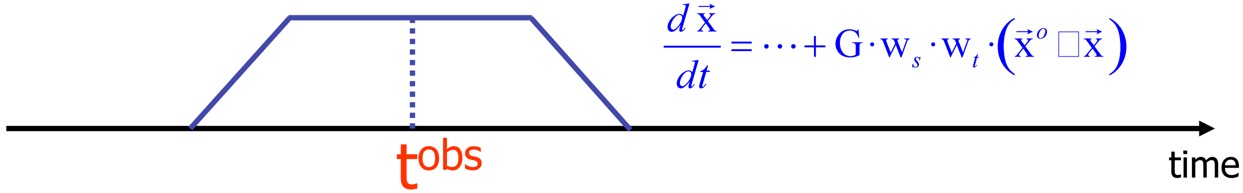

$$\frac{d\vec{x}}{dt} = \cdots + G \cdot w_s \cdot w_t \cdot \left(\vec{x}^o \square \vec{x}\right)$$

EnKF:

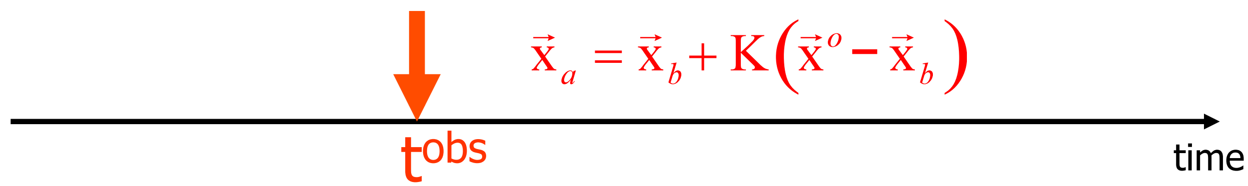

$$\vec{x}_a = \vec{x}_b + K\left(\vec{x}^o - \vec{x}_b\right)$$

Hybrid Nudging - EnKF:

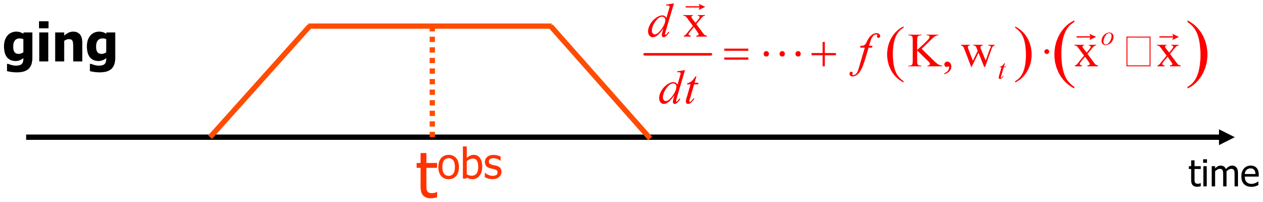

$$\frac{d\vec{x}}{dt} = \cdots + f\left(K, w_t\right) \cdot \left(\vec{x}^o \square \vec{x}\right)$$

- **The hybrid nudging coefficients:**

$$\frac{d\vec{x}}{dt} = \quad \cdots \quad + G \cdot w_s \cdot w_t \cdot \left(\vec{x}^o - \vec{x}\right)$$

$$G \cdot w_s = \frac{1}{\sum_t w_t \cdot \Delta t} \cdot K$$

Cannot say enough about judicious use of knowledge gained from the shallow water equations…

Hybrid Nudging - EnKF in 2D Shallow Water Model (SWM)

- The 2D shallow water equations… and hybrid nudging terms :

$$\frac{\partial u}{\partial t}+u\frac{\partial u}{\partial x}+v\frac{\partial u}{\partial y}-fv=-g\frac{\partial h}{\partial x}+\kappa\nabla^2 u+G_{uu}\cdot w_t\cdot\left(u^o-u\right)+G_{uv}\cdot w_t\cdot\left(v^o-v\right)+G_{uh}\cdot w_t\cdot\left(h^o-h\right)$$

$$\frac{\partial v}{\partial t}+u\frac{\partial v}{\partial x}+v\frac{\partial v}{\partial y}+fu=-g\frac{\partial h}{\partial y}+\kappa\nabla^2 v+G_{vu}\cdot w_t\cdot\left(u^o-u\right)+G_{vv}\cdot w_t\cdot\left(v^o-v\right)+G_{vh}\cdot w_t\cdot\left(h^o-h\right)$$

$$\frac{\partial h}{\partial t}+u\frac{\partial h}{\partial x}+v\frac{\partial h}{\partial y}=-h\left(\frac{\partial u}{\partial x}+\frac{\partial v}{\partial y}\right)+\kappa\nabla^2 h+G_{hu}\cdot w_t\cdot\left(u^o-u\right)+G_{hv}\cdot w_t\cdot\left(v^o-v\right)+G_{hh}\cdot w_t\cdot\left(h^o-h\right)$$

Diagonal (red) terms: traditional nudging

Hybrid Nudging - EnKF:
- Continuous Data Assimilation

2D Shallow Water Model (SWM) Results

(Lei and Stauffer 2009)

Quasi-Stationary Wave Case

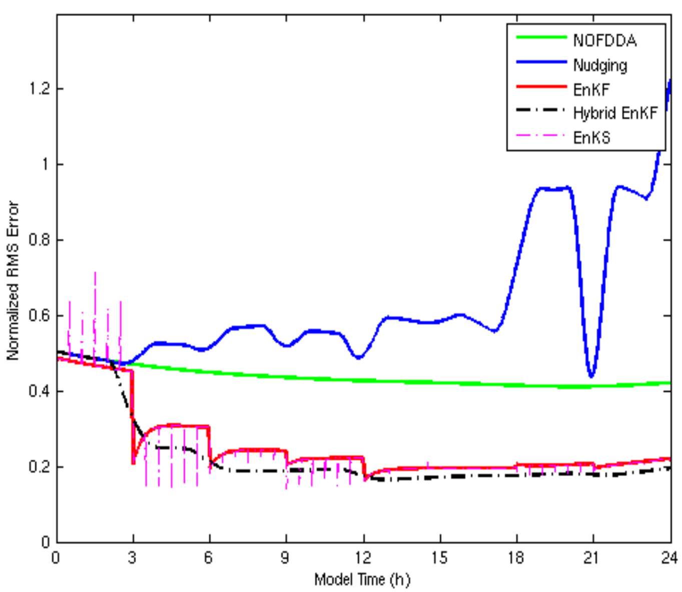

Moving Vortex Case

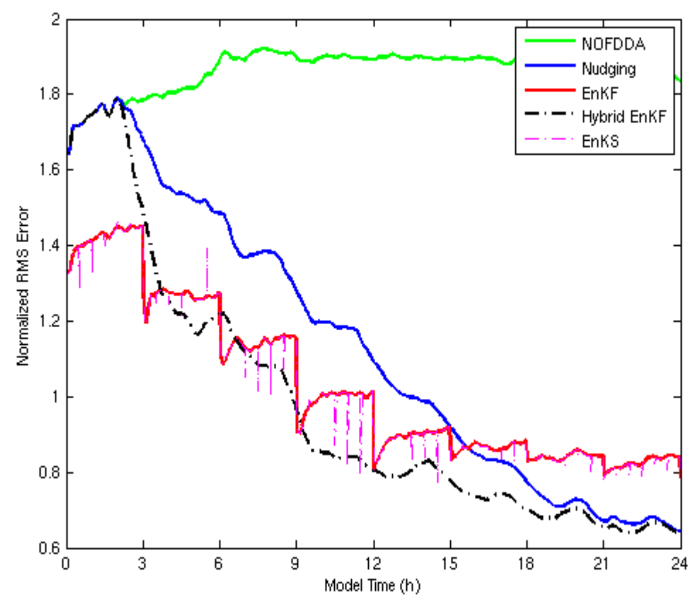

Extend Lorenz and SWM hybrid nudging – EnKF to 3D WRF / DART…

Methodology for the HNEnKF

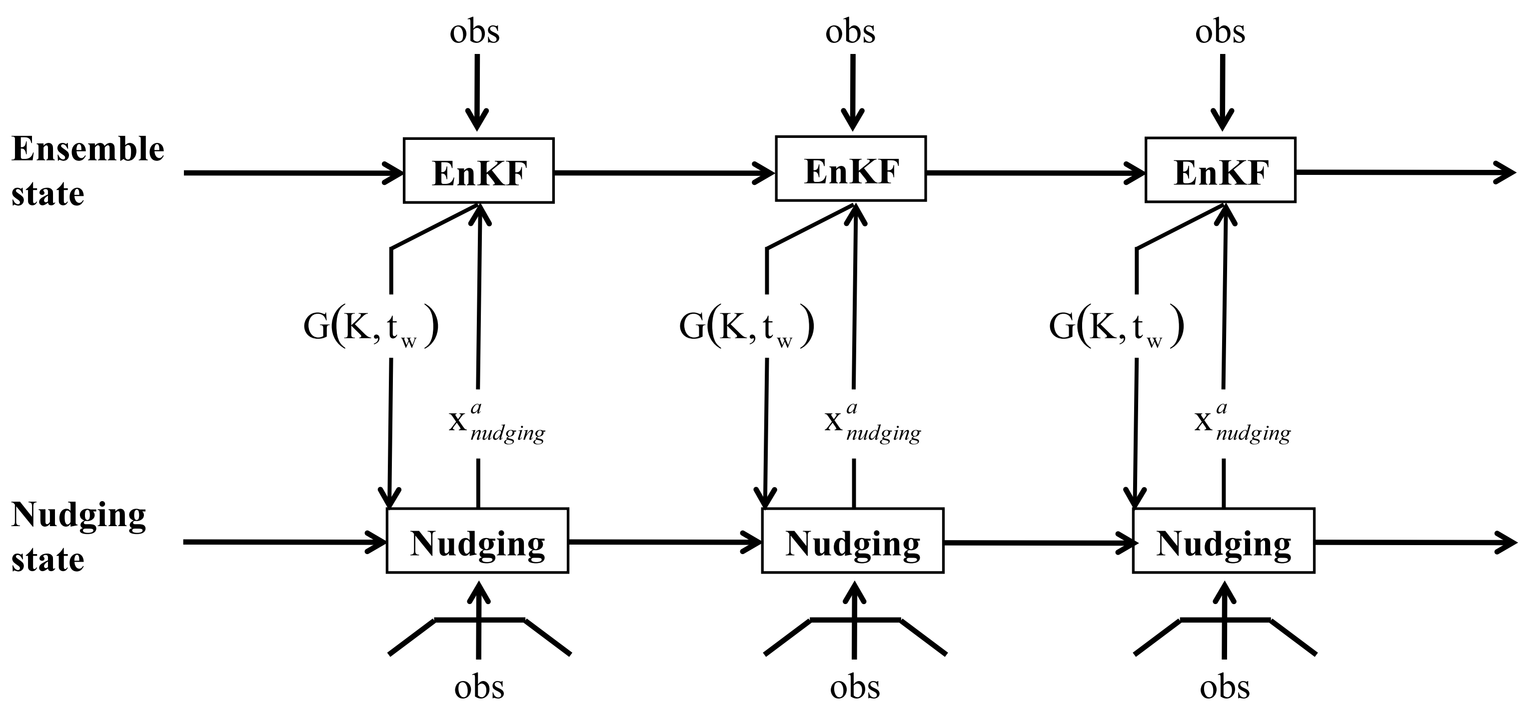

WRF/DART Ensemble Configurations

- IC ensemble: contains perturbations of the ICs and LBCs.
  - Adding perturbations, which are drawn from a multivariate normal distribution by use of the WRF-3DVAR, to the ICs and LBCs.
  - Ensemble size is 24 or 48
- ICPH ensemble: contains multi-physics members in addition to the perturbed ICs and LBCs members
  - Eight physics configurations are used
  - Ensemble size is 24 or 48

Physics configuration	Microphysics	Convective	PBL
1	WSM-3	Kain-Fritsch	MYJ
2	Lin et al.	Kain-Fritsch	MYJ
3	WSM-3	Betts-Miller-Janjic	MYJ
4	WSM-3	Kain-Fritsch	YSU
5	Lin et al.	Betts-Miller-Janjic	MYJ
6	Lin et al.	Kain-Fritsch	YSU
7	WSM-3	Betts-Miller-Janjic	YSU
8	Lin et al.	Betts-Miller-Janjic	YSU

(Lei and Stauffer 2011)

Experimental design

Exp. Name	Exp. Description
CTRL	Assimilate no observations
FDDA	Assimilate observations by observation nudging
EnKFIC24	Assimilate observations by EnKF with IC ensemble and 24 ensemble members
EnKFIC48	Assimilate observations by EnKF with IC ensemble and 48 ensemble members
EnKFICPH24	Assimilate observations by EnKF with ICPH ensemble and 24 ensemble members
EnKFICPH48	Assimilate observations by EnKF with ICPH ensemble and 48 ensemble members
HNEnKFIC24	Assimilate observations by HNEnKF with IC ensemble and 24 ensemble members
HNEnKFIC48	Assimilate observations by HNEnKF with IC ensemble and 48 ensemble members
HNEnKFICPH24	Assimilate observations by HNEnKF with ICPH ensemble and 24 ensemble members
HNEnKFICPH48	Assimilate observations by HNEnKF with ICPH ensemble and 48 ensemble members

Overview of the 18-20 September 1983 CAPTEX-83 (tracer) case

(a) 2200 UTC 18 September

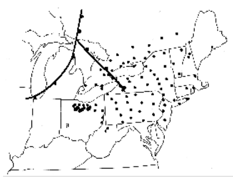

(b) 0400 UTC 19 September

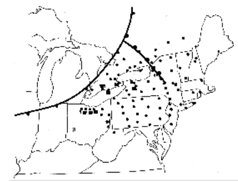

(c) 1000 UTC 19 September

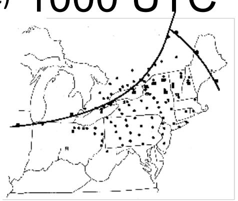

(d) 1600 UTC 19 September

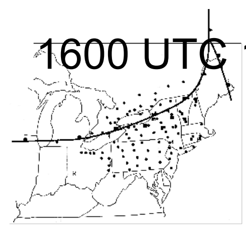

(After Deng et al. 2004)

Evaluation of temporal smoothness and insertion noise for IC ensemble

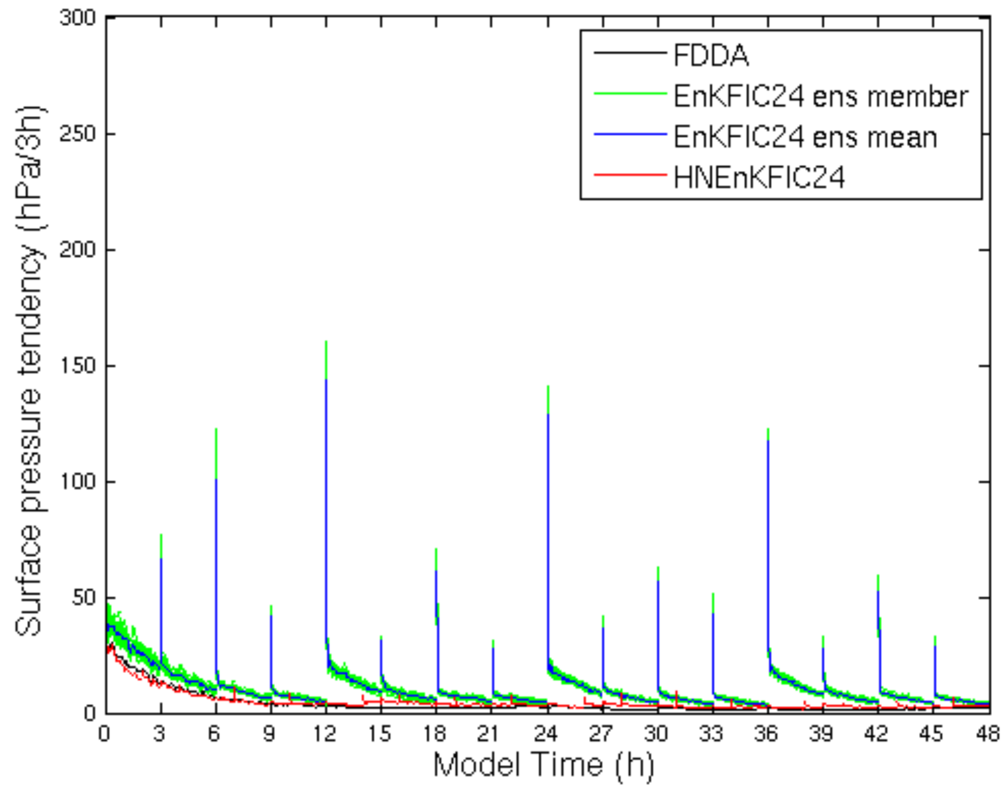

Evaluation of temporal smoothness and insertion noise for IC and ICPH ensembles

EnKF

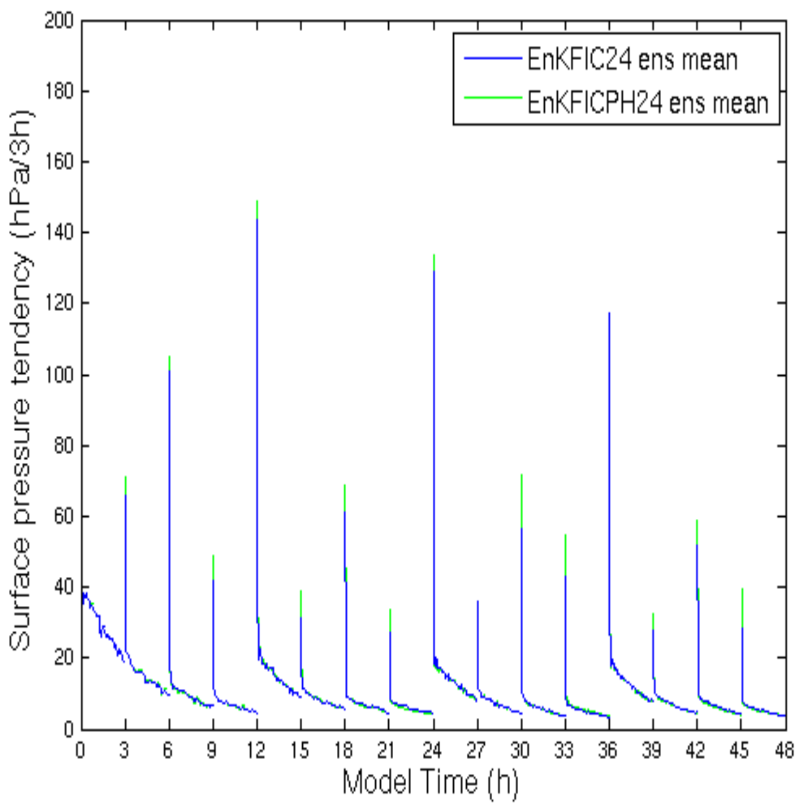

HNEnKF

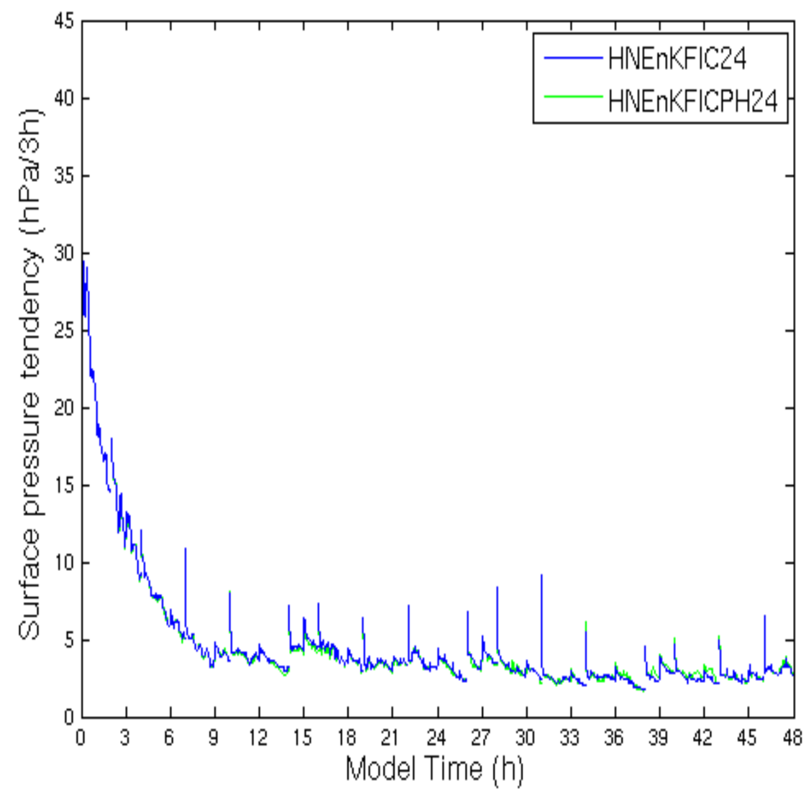

Evaluation using independent surface tracer data

Ordinal ranking	Experiment	Sum of misses and false alarms
1	FDDA	20
2	HNEnKFICPH24	21
2	HNEnKFICPH48	21
3	HNEnKFIC24	22
4	HNEnKFIC48	24
5	EnKFIC48	26
6	EnKFIC24	27
7	EnKFICPH24	31
7	EnKFICPH48	31
7	CTRL	31

Ensembles: Quantifying Uncertainty (Walter Kolczynski)

- Meteorological (MET) errors have important implications to many weather applications (e.g., AT&D, TDAs)
- Ensemble of AT&D models attractive but not practical for operations
- Efficient way to compute MET uncertainty from an NWP ensemble for input into a single AT&D model solution (HPAC/SCIPUFF wind variance matrices, UUE, VVE, UVE)
- NWP-ensemble variance (spread) is at best an approximate measure of actual uncertainty/error variance...

Motivation

- Can a single AT&D prediction using NWP-ensemble derived MET fields and wind variances (uncalibrated or calibrated) approximate and improve upon an AT&D prediction based on an explicit AT&D ensemble?
- Can we develop a simple calibration that will better predict the actual error variance?

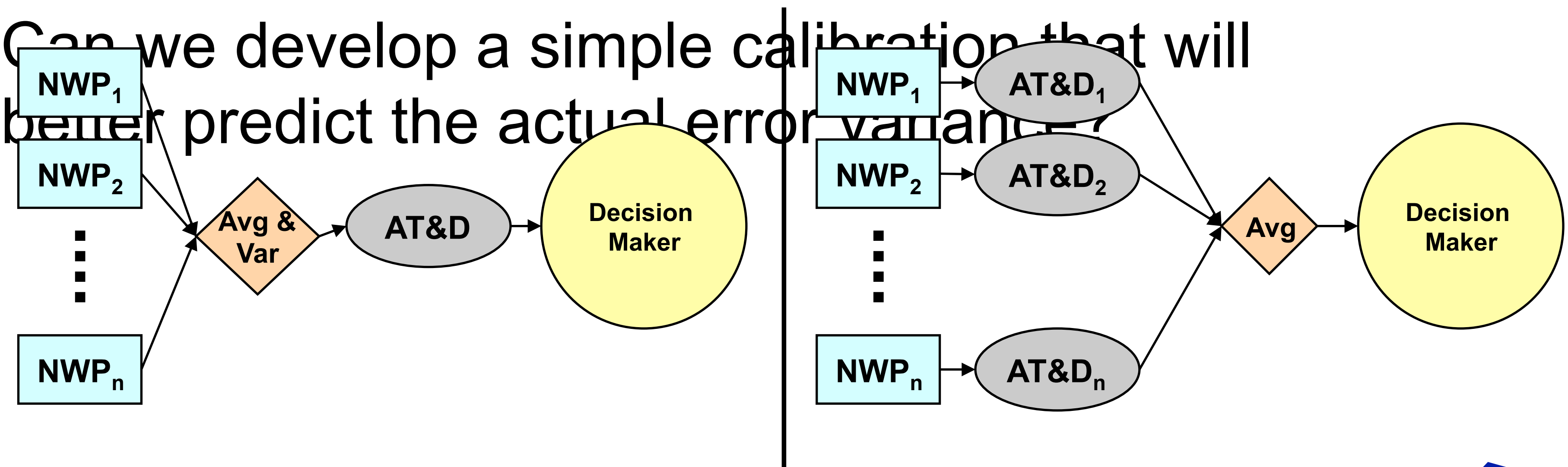

Linear Variance Calibration (LVC) Methodology

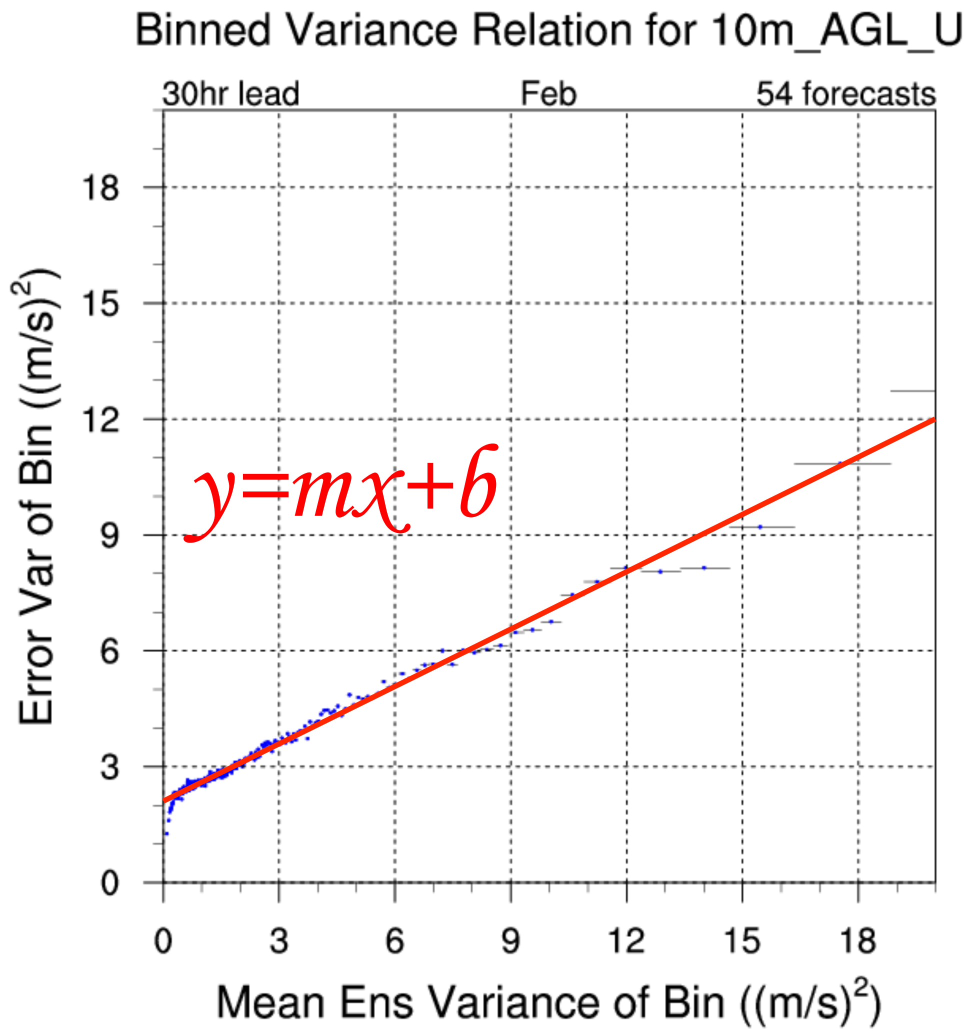

Daily MET-SCIPUFF Ensemble Testbed Overview

- Use 21 NCEP 32-km SREF members (ARW, NMM, ETA, RSM) over suitably long periods (~ 1 year)
- Run 21 SCIPUFF dispersion calculations
  - Combine dosage statistics (explicit ensemble)
- Run SCIPUFF using 4-km MM5 FDDA to generate “ground truth” dispersion
- Process SREF outputs for mean ensemble MET and MET uncertainty (wind variances)
- Run single 24-h 32-km SCIPUFF with ensemble MET uncertainty wind variances (SREF hazard prediction)
- Compare single-SCIPUFF SREF hazard prediction with 32-km explicit SCIPUFF ensemble using probabilistic verification and “ground truth” dispersion calculations

SREF Member Mean Dosages

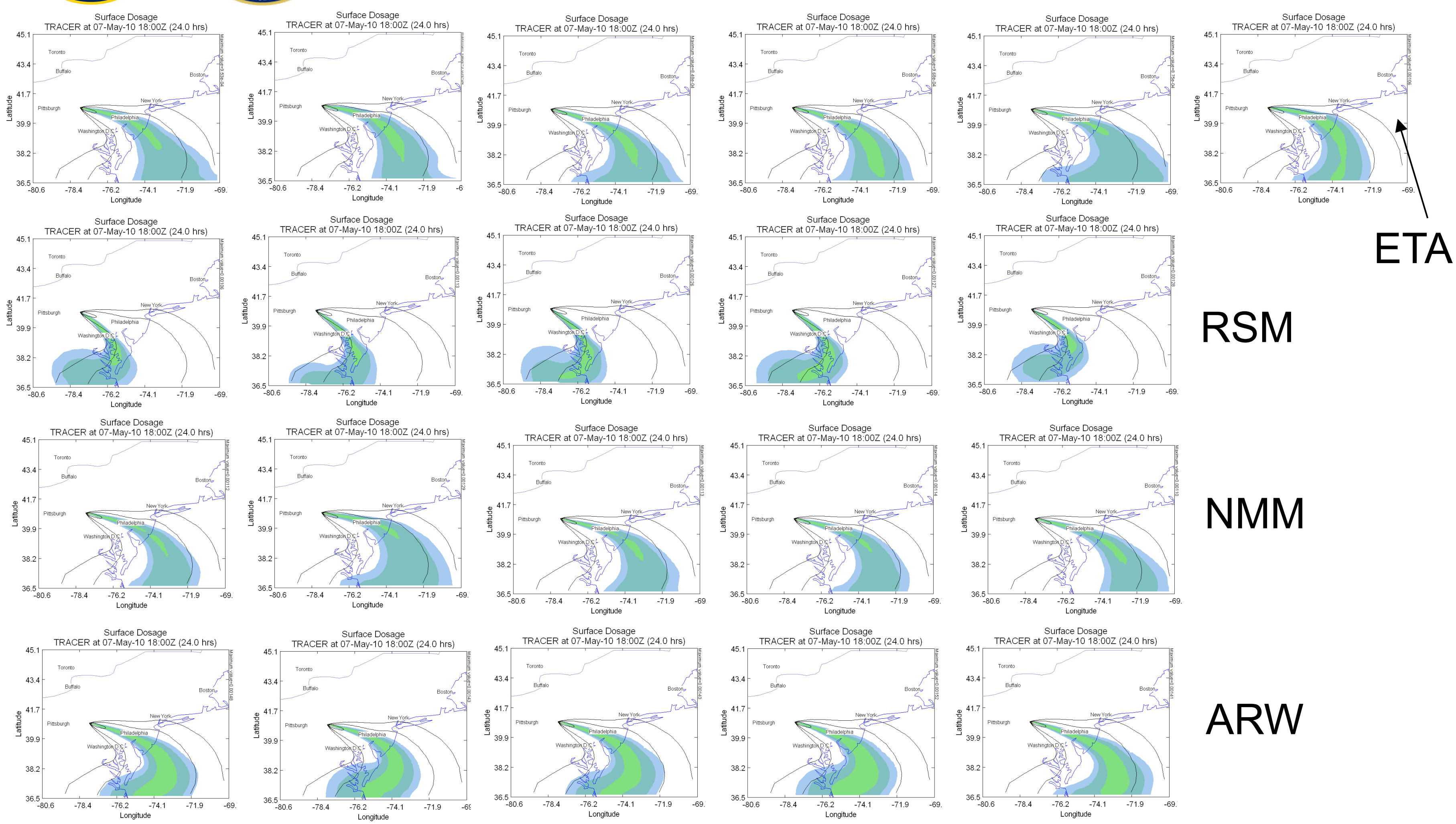

Mean Dosage and Comparison

SREF Ensemble Average

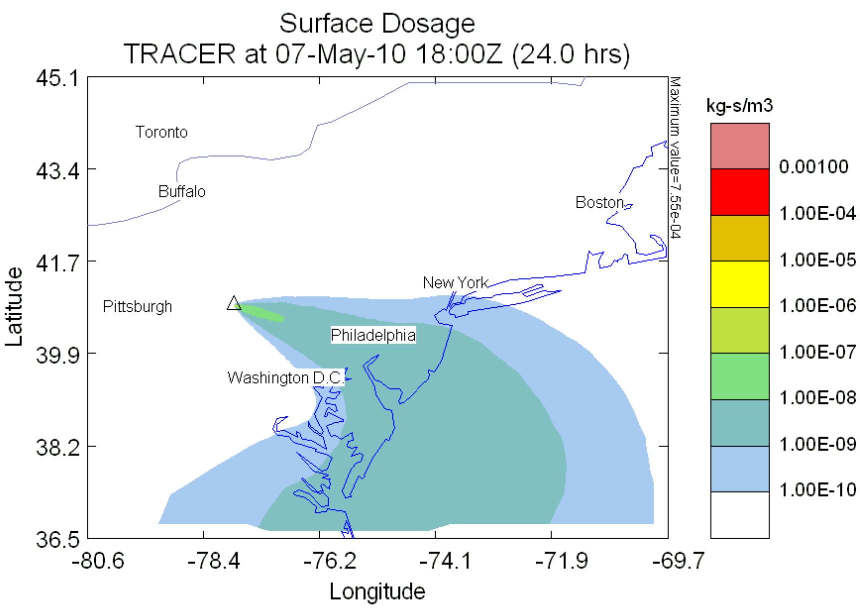

MM5 Truth (color) + SREF Ensemble Probability>1.0E-9

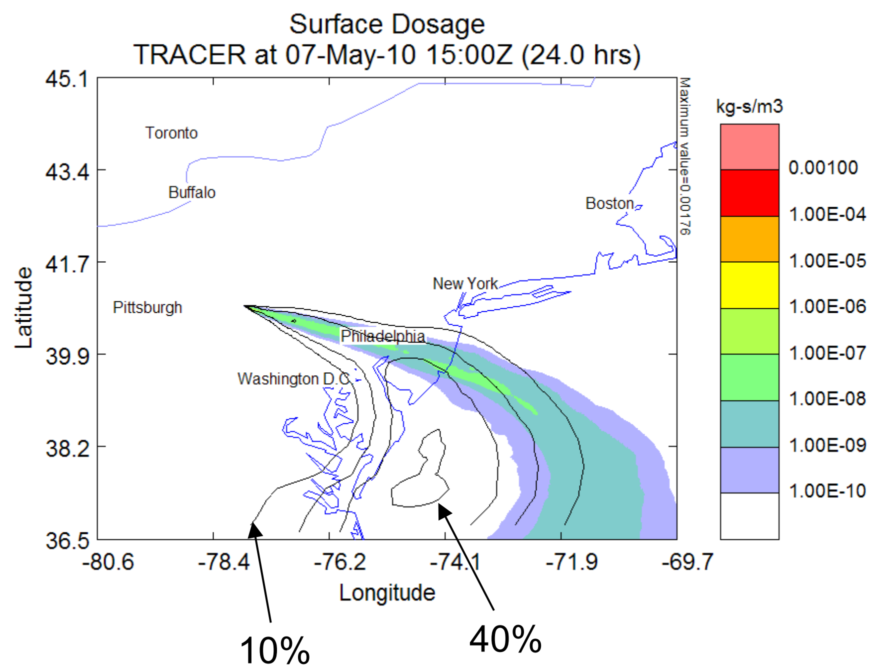

Sample Reliability

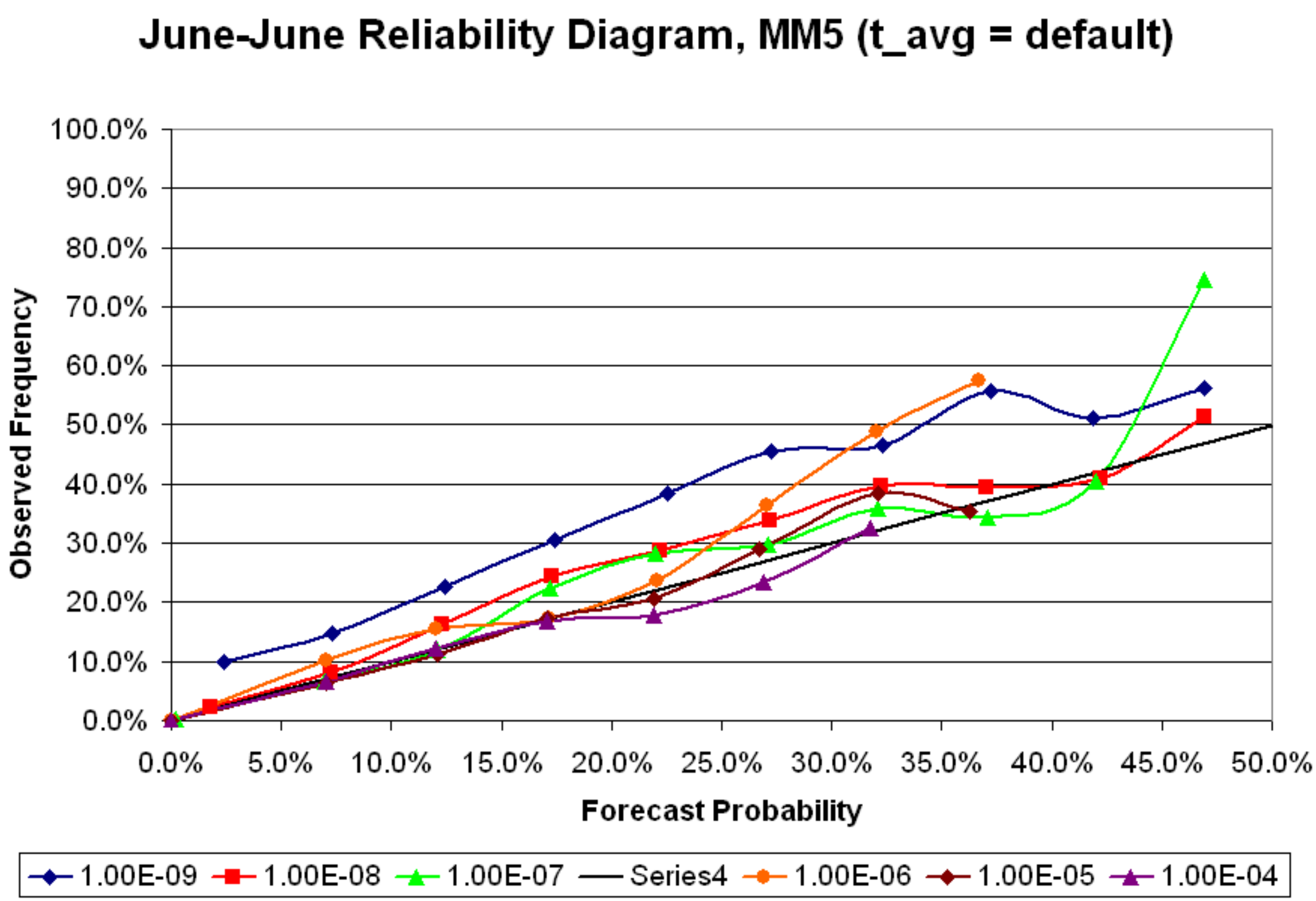

PENNSTATE

1855

488 JOURNAL OF APPLIED METEOROLOGY VOLUME 41

Ensemble Simulations with Coupled Atmospheric Dynamic and Dispersion Models: Illustrating Uncertainties in Dosage Simulations

THOMAS T. WARNER,[*,#] RONG-SHYANG SHEU,[*] JAMES F. BOWERS,[@] R. IAN SYKES,[&] GREGORY C. DODD,[**] AND DOUGLAS S. HENN[&]

[*]*National Center for Atmospheric Research,*[+] *Boulder, Colorado*
[#]*Program in Atmospheric and Oceanic Sciences, University of Colorado, Boulder, Colorado*
[@]*U.S. Army West Desert Test Center, Dugway, Utah*
[&]*ARAP Group, Titan Research & Technology, Princeton, New Jersey*
[**]*H.E. Cramer Co., Inc., Sandy, Utah*

(Manuscript received 20 March 2001, in final form 31 October 2001)

DEPARTMENT OF
METEOROLOGY
COLLEGE OF EARTH AND
MINERAL SCIENCES

PENNSTATE

1855

VOLUME 48 JOURNAL OF APPLIED METEOROLOGY AND CLIMATOLOGY OCTOBER 2009

Ensemble Variance Calibration for Representing Meteorological Uncertainty for Atmospheric Transport and Dispersion Modeling

WALTER C. KOLCZYNSKI JR., DAVID R. STAUFFER, SUE ELLEN HAUPT, AND AIJUN DENG

Department of Meteorology, The Pennsylvania State University, University Park, Pennsylvania

(Manuscript received 17 June 2008, in final form 22 January 2009)

DEPARTMENT OF
METEOROLOGY
COLLEGE OF EARTH AND MINERAL SCIENCES

Investigation of Ensemble Variance as a Measure of True Forecast Variance

Walter C. Kolczynski, Jr.[1]*, David R. Stauffer[1], Sue Ellen Haupt[1], Naomi S. Altman[2]

and Aijun Deng[1]

The Pennsylvania State University
University Park, PA 16802

[1] Department of Meteorology
[2] Department of Statistics

For Submission to Monthly Weather Review

December 2010

Revised May 2011

*Corresponding author: phone: 814-863-1036, e-mail: wck122@psu.edu

PENNSTATE

Mean Absolute Reliabilty Error (MARE)

Concentration (~100 cases, min 20 forecasts)

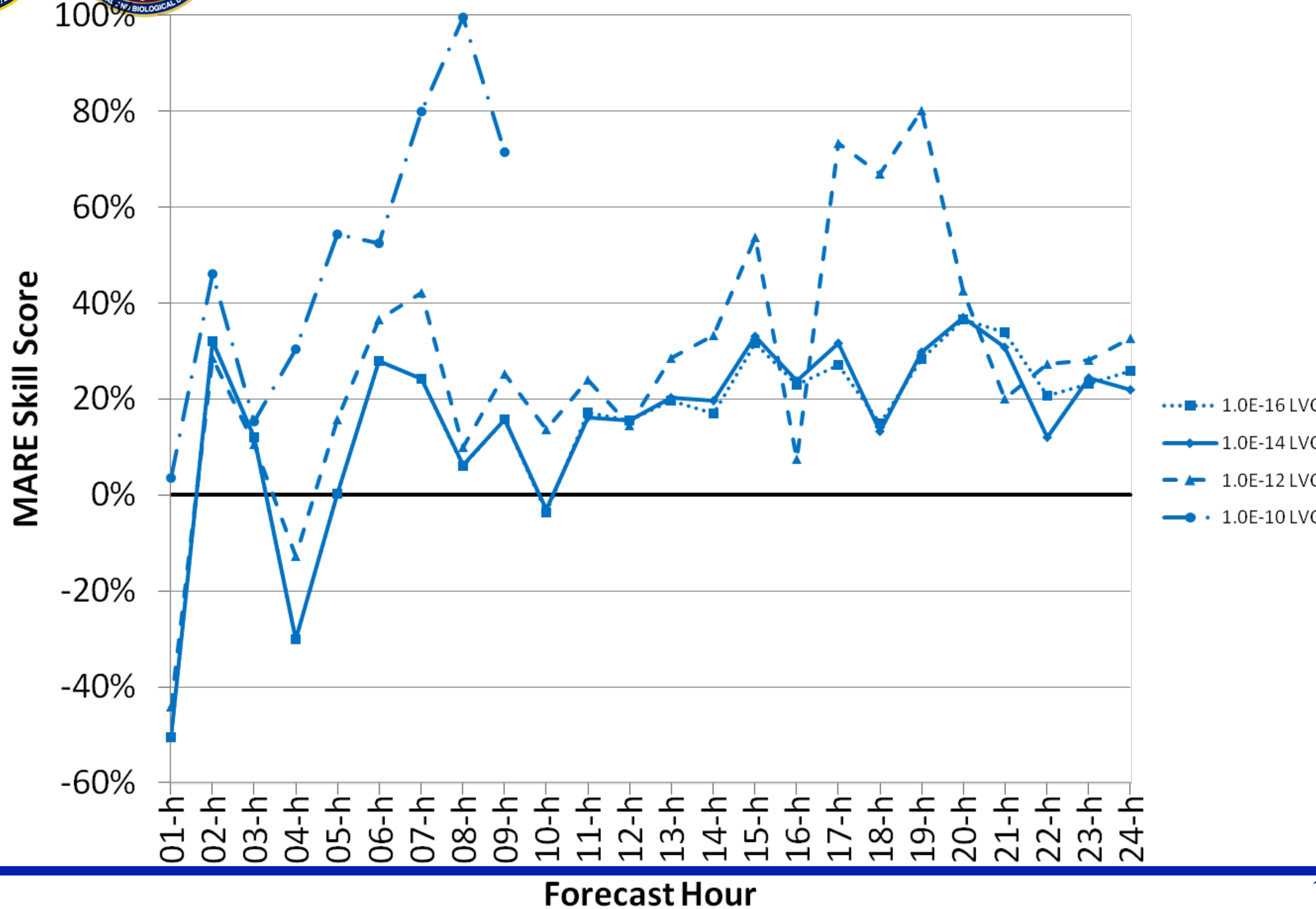

Walter Kolczynski, Jr., new Ph.D

Thank-you !!!

DEPARTMENT OF
METEOROLOGY
COLLEGE OF EARTH AND MINERAL SCIENCES

PENNSTATE

Supplementary Slides

Methodology for the HNEnKF

Model equation with additional nudging terms:

$$\frac{d\mathbf{x}}{dt} = f\left(\mathbf{x}\right) + \mathbf{G} \cdot \mathrm{w}_s \cdot \mathrm{w}_t \cdot \left(\mathbf{y}^o - \mathbf{H}\mathbf{x}\right)$$

Hybrid nudging coefficients:

$$\mathbf{G} \cdot \mathrm{w}_s = \frac{1}{\left(\sum_{t=t^o-\tau_N}^{t^o} \mathrm{w}_t \cdot \Delta t\right)} \approx \mathbf{K}$$

- The hybrid nudging coefficients come directly from the EnKF gain matrix **K** that contains information from the flow-dependent background error covariances computed from an ensemble forecast.
- Thus there is no need to specify the nudging strength or the spatial nudging weighting coefficient in either the horizontal or vertical directions.
- The hybrid nudging terms include not only the standard diagonal terms (i.e., u correction in u-equation, v correction in v-equation, etc.) in the nudging magnitude matrix **G**, but also the off-diagonal terms (i.e., inter-variable influence).
- This statistical inter-variable influence is included in the model's relaxation terms to gradually and continuously force the model towards the observations.
- Thus the error spikes and dynamic imbalances often produced by intermittent EnKF are reduced.

Experiment design – parameters

Experiment	Nudging strength	Horizontal radius of influence	Surface data vertical radius of influence (stable PBL)	Surface data vertical radius of influence (unstable PBL)	Half-period of nudging time window	Horizontal error covariance localization	Vertical error covariance localization	Error covariance inflation
FDDA	4×10^{-4} s^{-1}	67-200 km	100 m	PBL top plus 50m	1-2 h	---	---	---
EnKF	---	---	---	---	---	533 km	150 hPa	Adaptive inflation
HNEnKF	---	---	---	---	1-2 h	533 km	150 hPa	Adaptive inflation

Observations Research Progress: Characteristics vs. Speed; 6-hr Ave, Spring, Summer, Fall 2009

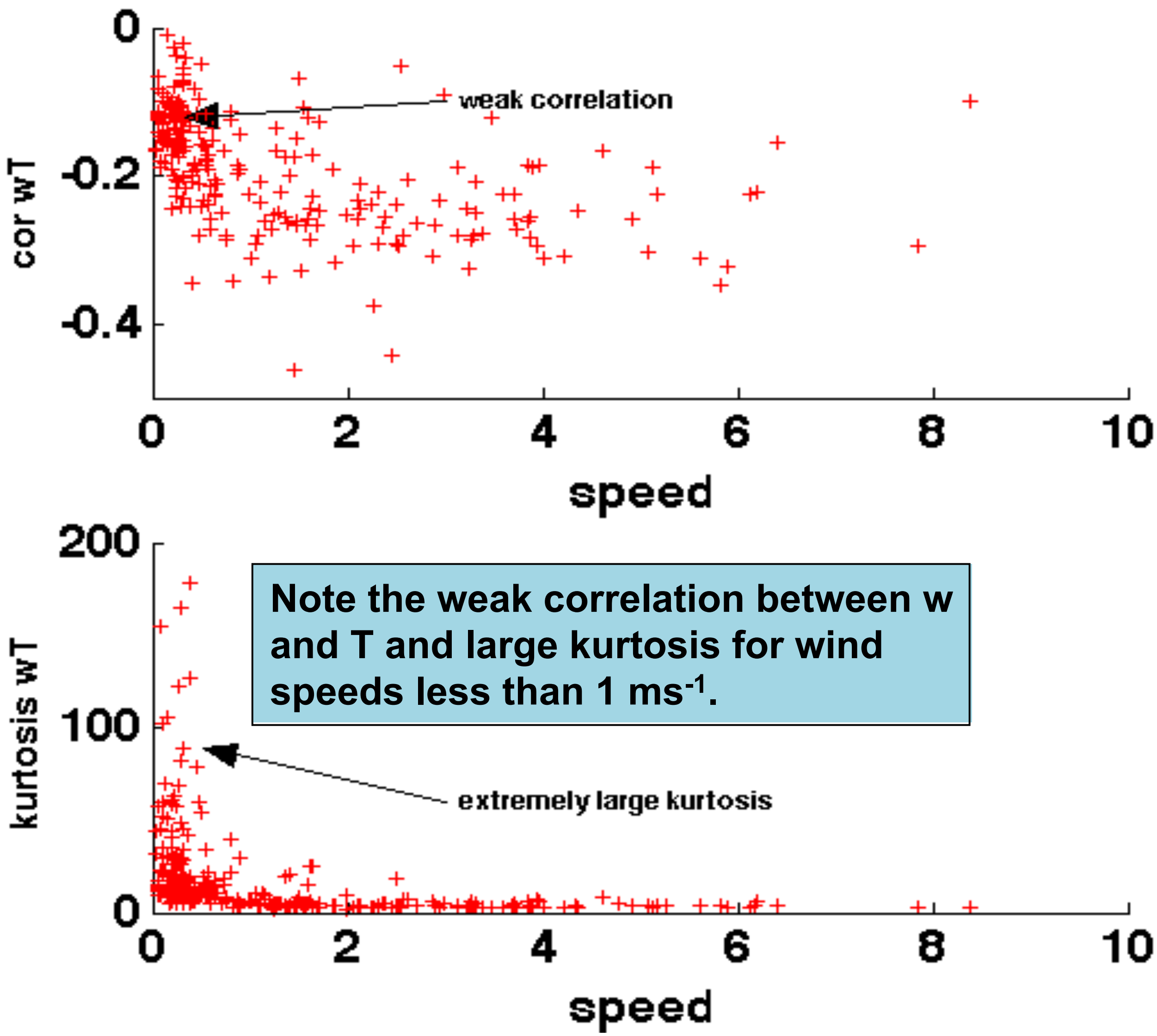

Note the weak correlation between w and T and large kurtosis for wind speeds less than 1 ms^{-1}.

DEPARTMENT OF METEORC
COLLEGE OF MINERA

Probability Distribution of One-minute Averages of 5-s Heat Fluxes at Rock Springs for the Very Weak Wind, Highly Stable Regime

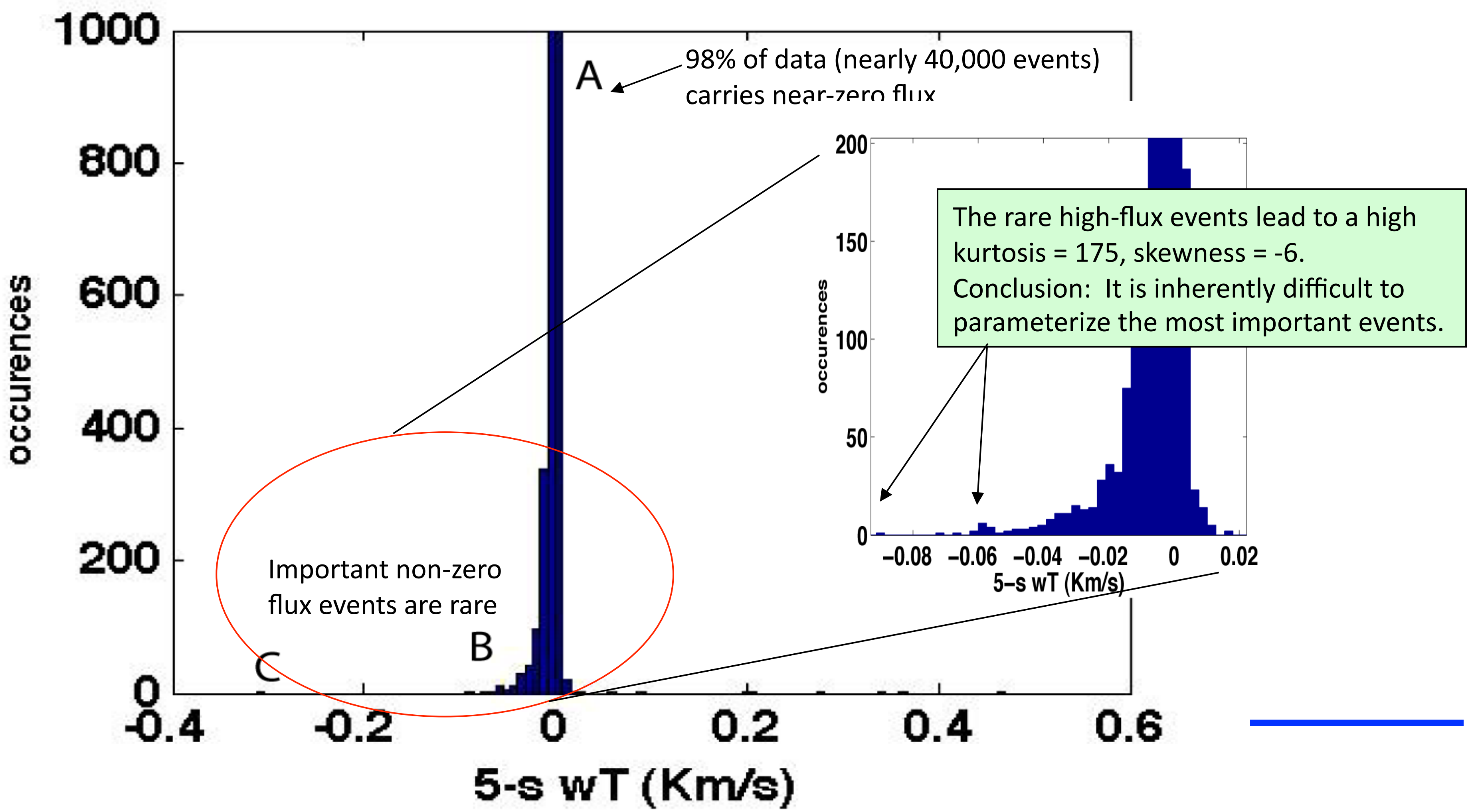

PENNSTATE

One Min. Averaged Sigma_w and Scaled Sigma_w for Near-calm Nights with Strong Averaged Stratification (Black) and Weaker Stratification (Red) as a Function of Rb

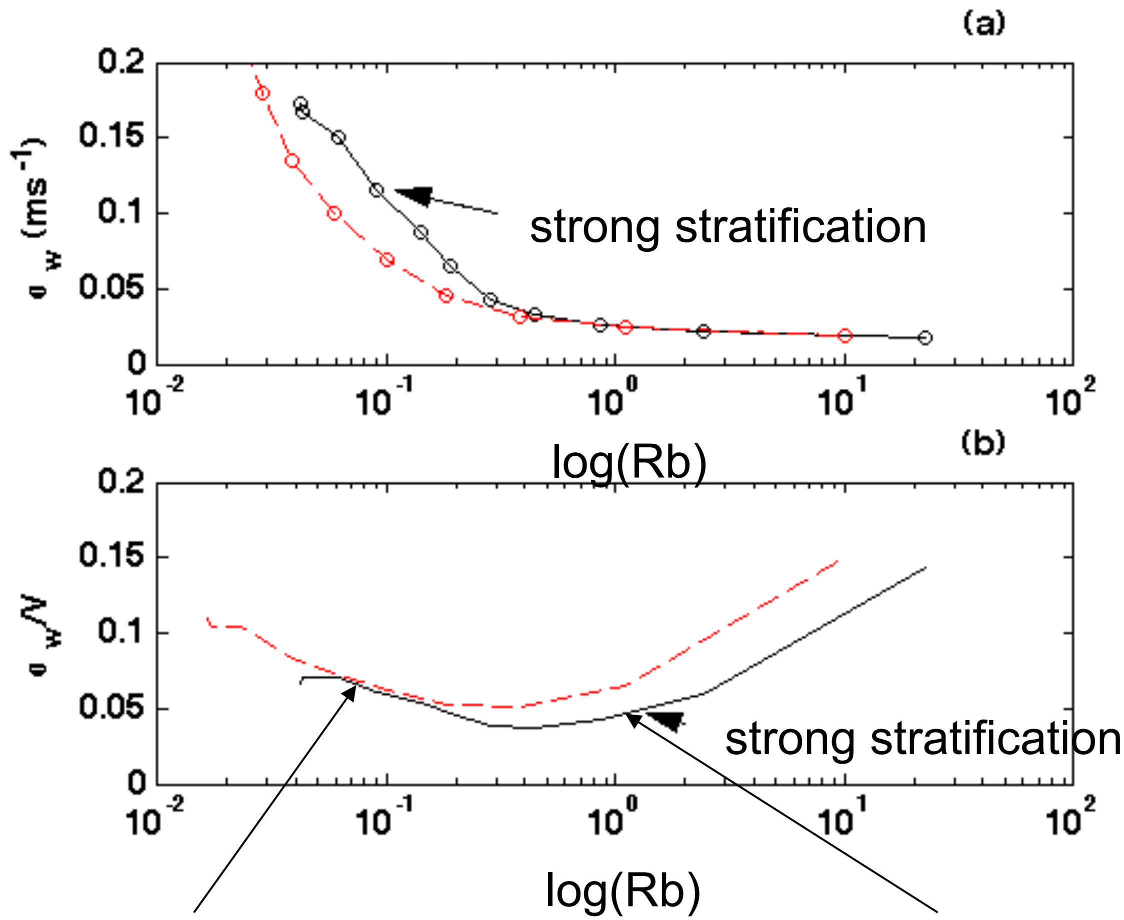

Similarity Theory Valid for Weak Stability

Similarity Theory Fails for Stronger Stability

DEPARTMENT OF
METEOROLOGY
COLLEGE OF EARTH AND MINERAL SCIENCES

Sensitivity of Parcel Trajectories to Model Resolution & PBL Physics

Time: 0800 – 1112 UTC **Case: 7 Oct. 2007**

Exp. Baseline

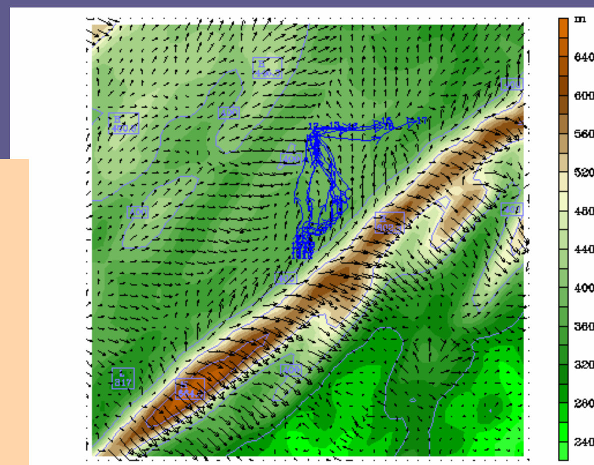

Exp. Modified PBL Physics

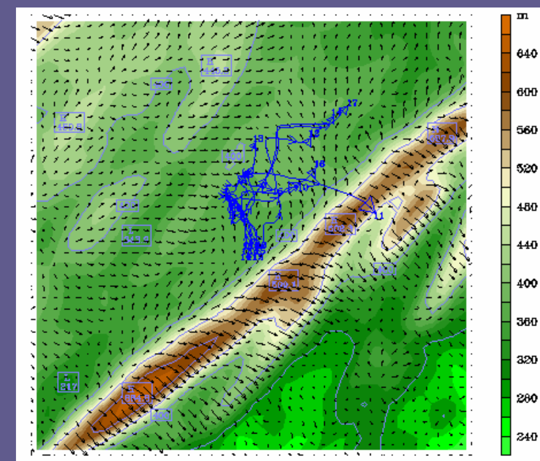

Exp. LrgDX

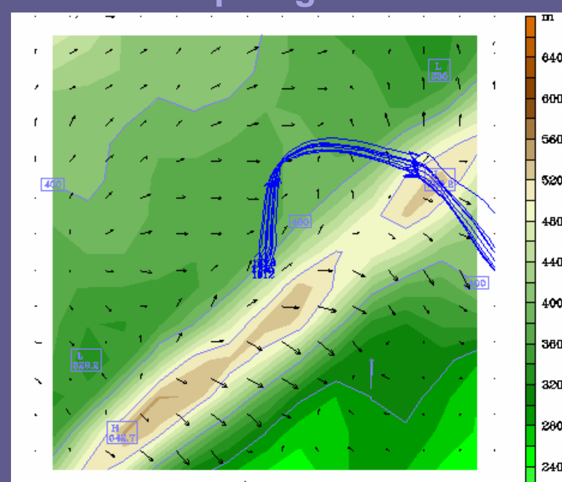

Exp. LrgDZ

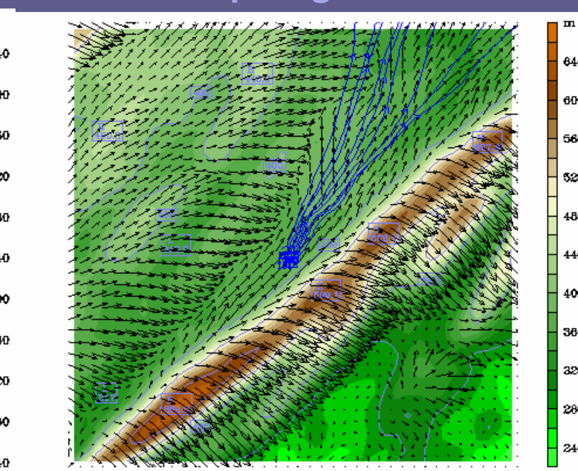

Trajectory Sensitivity:

- **Reduced mixing in modified PBL physics allows more sub-meso motions and inter-parcel variability.**

- **Lower 1.3-km horizontal resolution produces larger speed bias.**

- **Lower standard vertical resolution suppresses gravity-driven slope flows.**

Surface Dosage at 3 h Following Release and Valid at 11 UTC

SCIPUFF Sensitivity:

- **Reduced mixing in MYJ-mod allows more sub-meso motions and greater dispersion.**
- **Lower horizontal resolution produces larger speed bias, less-resolved drainage flow and less lateral (cross-plume) dispersion.**
- **Lower vertical resolution suppresses gravity-driven slope flows and produces a plume more parallel to the mountain.**

Exp. Baseline

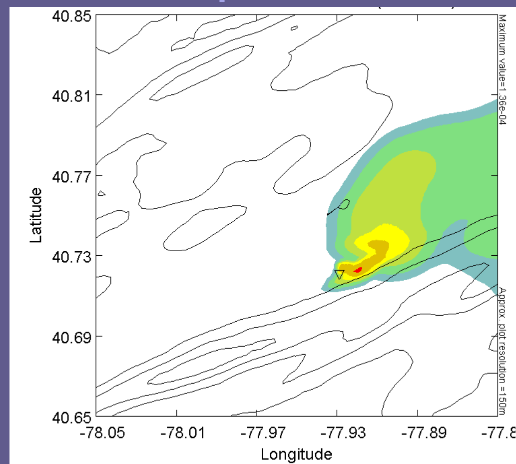

Exp. MYJ-mod

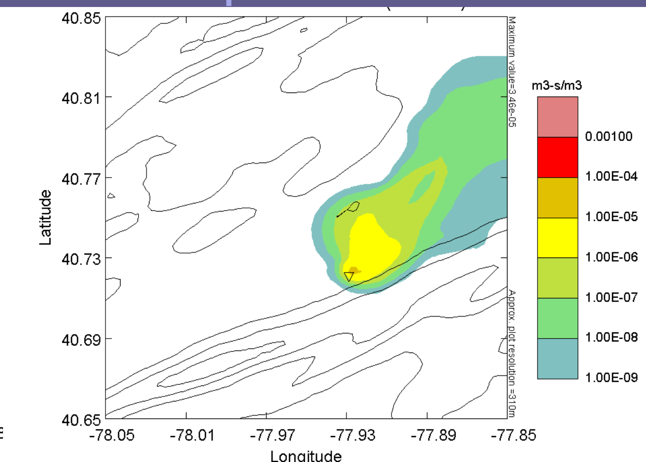

Exp. LrgDX

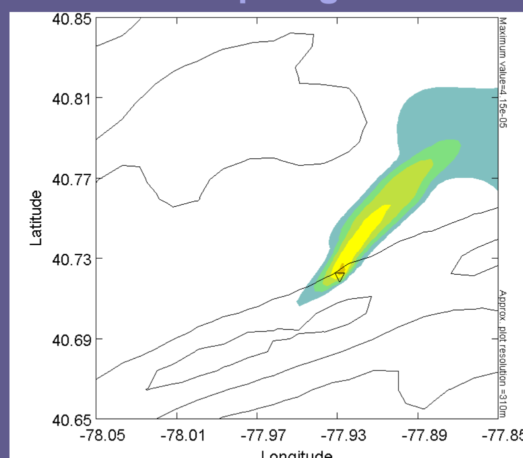

Exp. LrgDZ

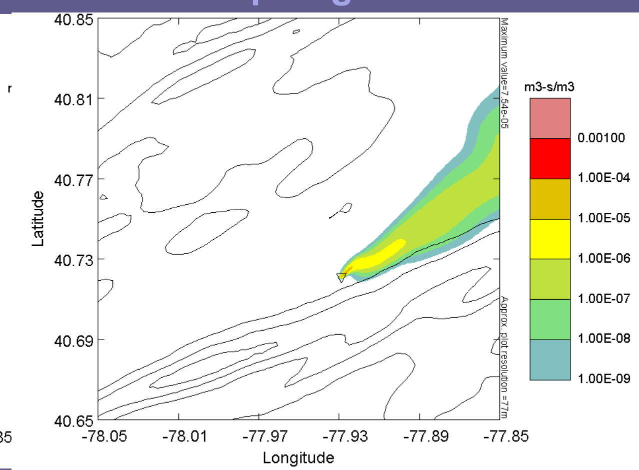

Modeling the Stable Boundary Layer and its Impact on Atmospheric Transport and Dispersion

M01-015

David R. Stauffer[1], Brian P. Reen[1], Astrid Suarez[1], Brian J. Gaudet[1], Joshua D. Hoover[1], Scott J. Richardson[1], Larry Mahrt[2], and Nelson L. Seaman[1]

[1] Dept. of Meteorology, Penn State University;[2] COAS, Oregon State University

WRF 0.444-km domain

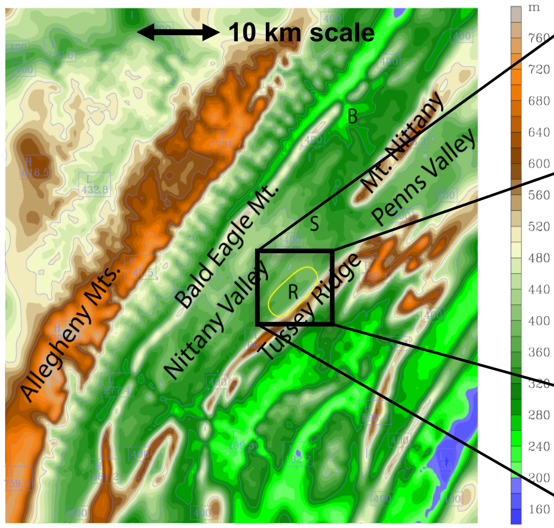

Observation Network

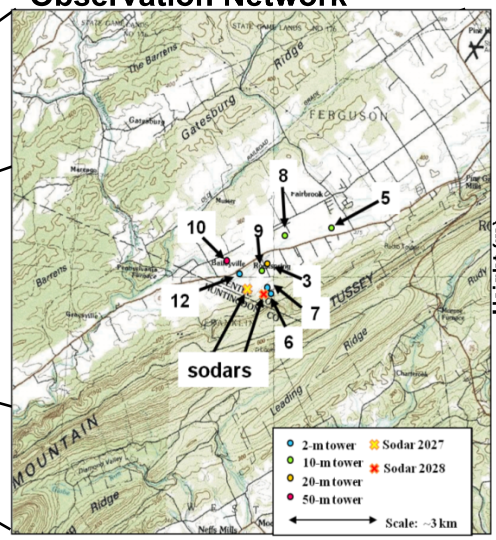

Comparison of sodar-measured winds with sonic-anemometer wind data at 50-m tower

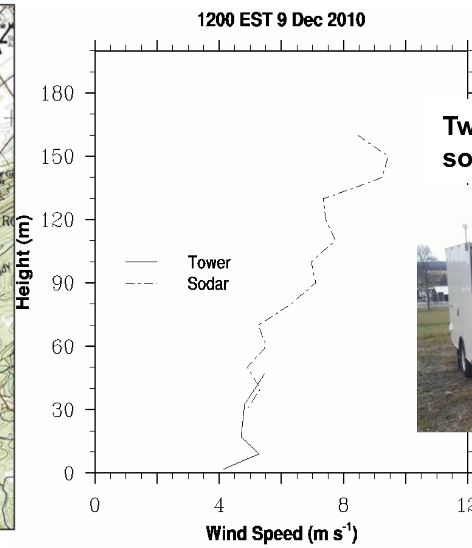

Two ARO-DURIP-funded sodars

The effect of terrain-induced gravity waves on hazard prediction is investigated using a **combined observation and modeling study** over the complex terrain of Central Pennsylvania.

Regions of wave reflection

Vertical Velocities (shaded) and θ (contoured) at 0836 UTC

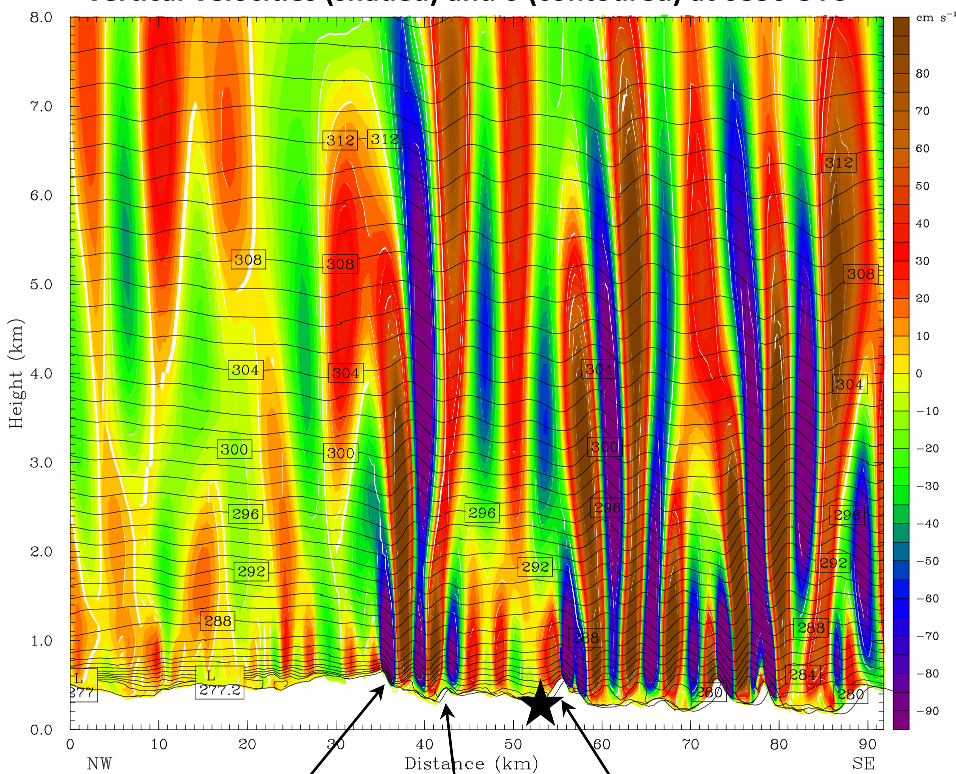

Vertical Profile of Vertical Wavenumber at Site 9

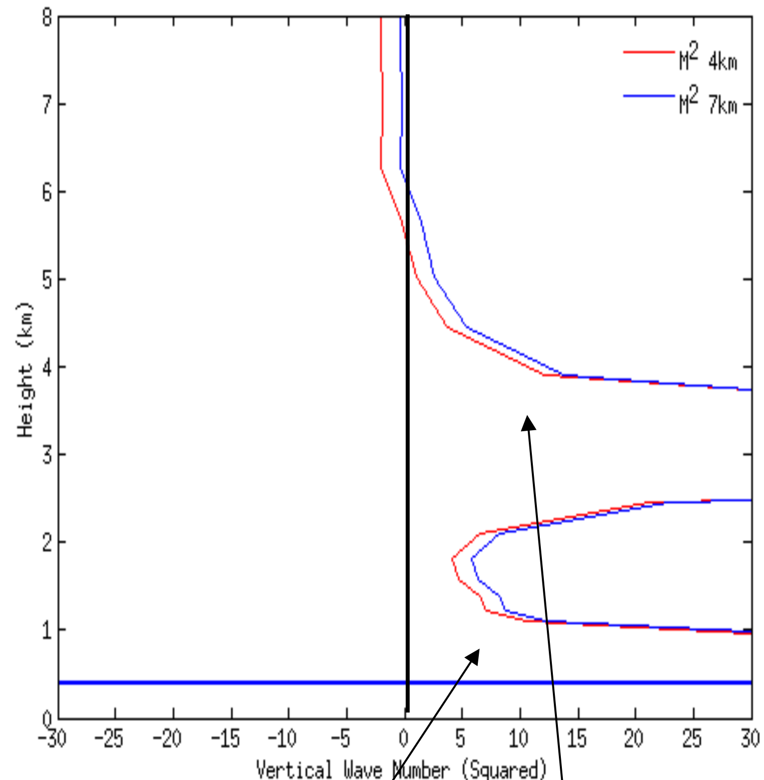

Regions where wave reflection is predicted by linear theory

Evaluation using independent surface tracer data

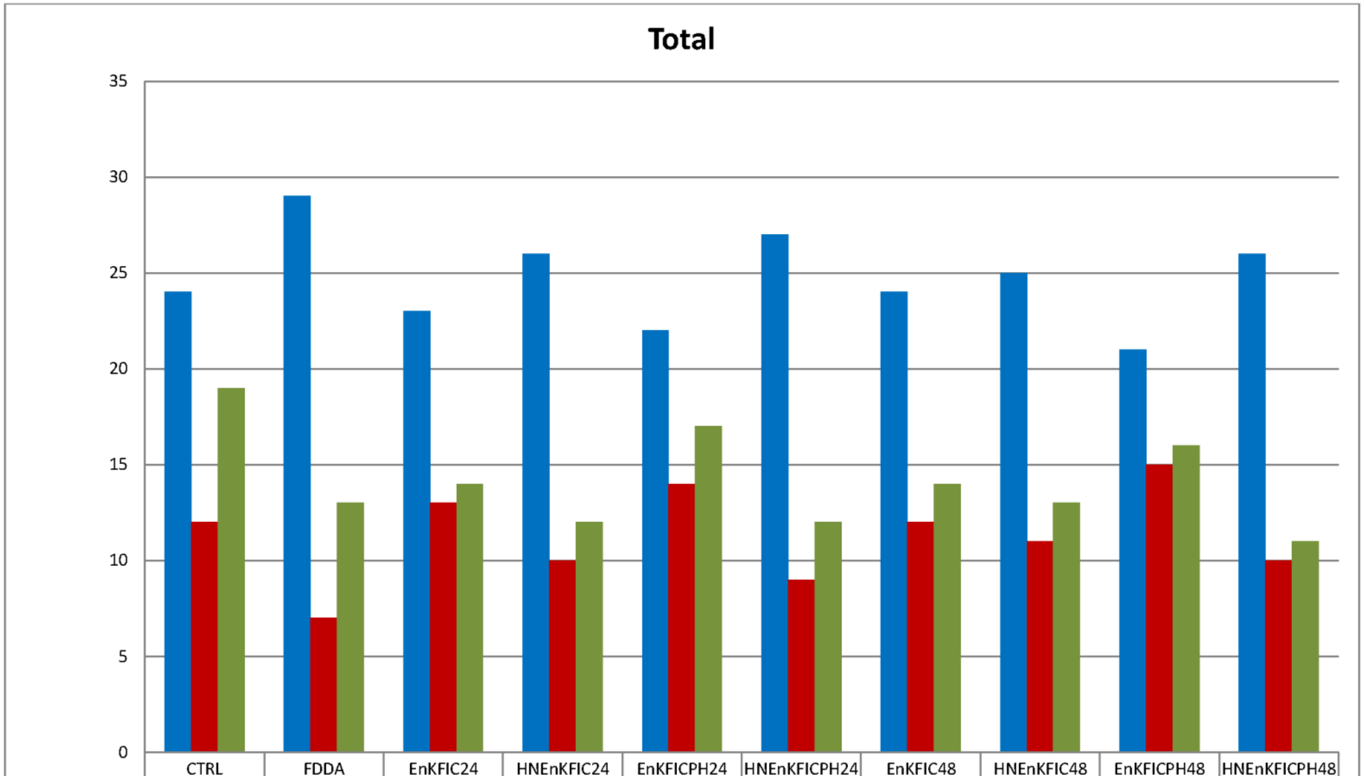

	CTRL	FDDA	EnKFIC24	HNEnKFIC24	EnKFICPH24	HNEnKFICPH24	EnKFIC48	HNEnKFIC48	EnKFICPH48	HNEnKFICPH48
Hit	24	29	23	26	22	27	24	25	21	26
Miss	12	7	13	10	14	9	12	11	15	10
FalseAlarm	19	13	14	12	17	12	14	13	16	11

The composite statistics (hits, misses and false alarms) through the 24-h period